
Article:
Hart, A. orcid.org/0000-0002-4433-5887, Porbenib, D.W., Omonmhenle, S. et al. (1 more author) (2023) Waste bone char-derived adsorbents: characteristics, adsorption mechanism and model approach. Environmental Technology Reviews, 12 (1). pp. 175-204. ISSN: 2162-2515

https://doi.org/10.1080/21622515.2023.2197128

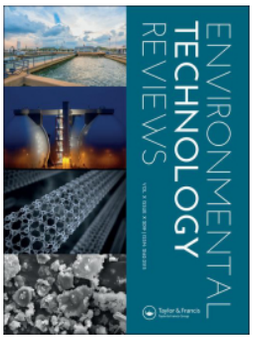

Environmental Technology Reviews

ISSN: 2162-2515 (Print) 2162-2523 (Online) Journal homepage: www.tandfonline.com/journals/tetr20

Waste bone char-derived adsorbents: characteristics, adsorption mechanism and model approach

Abarasi Hart, Duduna William Porbeni, Selina Omonmhenle & Ebikapaye Peretomode

To cite this article: Abarasi Hart, Duduna William Porbeni, Selina Omonmhenle & Ebikapaye Peretomode (2023) Waste bone char-derived adsorbents: characteristics, adsorption mechanism and model approach, Environmental Technology Reviews, 12:1, 175-204, DOI: 10.1080/21622515.2023.2197128

To link to this article: https://doi.org/10.1080/21622515.2023.2197128

Published online: 13 Apr 2023.

ENVIRONMENTAL TECHNOLOGY REVIEWS
2023, VOL. 12, NO. 1, 175–204
https://doi.org/10.1080/21622515.2023.2197128

Taylor & Francis
Taylor & Francis Group

REVIEW

OPEN ACCESS Check for updates

Waste bone char-derived adsorbents: characteristics, adsorption mechanism and model approach

Abarasi Hart[a], Duduna William Porbeni[b], Selina Omonmhenle[c] and Ebikapaye Peretomode[d]

[a]Department of Chemical and Biological Engineering, University of Sheffield, Sheffield, UK; [b]Department of Chemical Engineering, Niger Delta University, Wilberforce Island, Nigeria; [c]Department of Chemistry, Faculty of Physical Sciences, University of Benin, Benin, Nigeria; [d]School of Engineering, Robert Gordon University, Aberdeen, UK

ABSTRACT

The increase in meat consumption will result in a significant amount of bone being generated as solid waste and causing pollution to the environment. By pyrolysis or gasification, waste bones can be converted into bone char (BC), which can be used as an adsorbent for removing pollutants from wastewater and effluent gas. The purpose of this study is to critically appraise results from pertinent research and to collect and analyse data from studies on BC adsorbent applications from experimental, semi-empirical, theoretical and contextual viewpoints. Detailed descriptions of the theoretical adsorption mechanism, as well as possible interactions between pollutants and BC surface, were provided for the removal of pollutants. The study provides insights into the effect of synthesis conditions on BC's physicochemical properties and strategies for improving its adsorption capacity as well as future outlooks to guide research and support the development of green and cost-effective adsorbent alternatives to tackle water pollution. Additionally, this review discusses the application of BC to remove contaminants from water and soil, outlines strategies for regenerating pollutant-saturated BC, interprets the adsorption kinetics and isotherm models used in BC sorption studies, and highlights large-scale applications using packed-bed columns. Consequently, we proposed that when selecting the optimum isotherm model, experimental data should be used to substantiate the theory behind the predicted isotherm. Therefore, error functions combined with non-linear regression are the most effective method for obtaining and selecting optimal parameter values for adsorption kinetics and isotherm models.

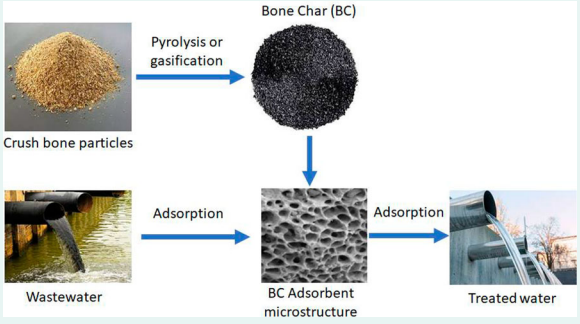

ARTICLE HISTORY
Received 6 November 2022
Accepted 19 March 2023

KEYWORDS
Bone char; adsorption; kinetics and isotherm models; regeneration; adsorption capacity enhancement

1. Introduction

Developing low-cost adsorbents for treating industrial effluents and wastewater has become a rising concern for environmental researchers. The removal of organic and inorganic contaminants from aqueous solutions is efficiently accomplished through adsorption. Physicochemically, adsorption occurs when contaminants accumulate on surfaces of porous solids due to their large internal surface area and surface chemistry. To date, a lot of research progress and efforts have been put into exploring waste bones, which opens up a new opportunity for wide-ranging applications, such as hydroxyapatite

CONTACT Abarasi Hart hartabarasi@yahoo.com, abarasi.hart@sheffield.ac.uk Department of Chemical and Biological Engineering, University of Sheffield, Sheffield S1 3JD, UK

for tissue engineering, hierarchical porous carbon for energy storage, phosphate source for soil remediation, heterogeneous catalyst and adsorbent for the treatment of contaminated gas, water and soil [1,2]. On one hand, adsorbents made of carbon are important in a variety of environmental technologies, including the purification and separation of gases, the purification of drinking water, the degradation of pollutants, the treatment of wastewater, and soil remediation [2,3]. In contrast, consumption of beef and meat is accumulating bones as solid waste, requiring proper solid waste management in order to eschew public health issues during decomposition of the organic content [1]. On the other hand, from an agro-environmental and economic perspective, the conversion of waste bone-to-materials, such as hydroxyapatite and bone char (BC) adsorbents is of great interest. The outstanding physicochemical properties of BC make it an ideal adsorbent for environmental pollution control [4]. Therefore, BC derived from waste bones for water treatment promotes a circular economy and is an effective method of reducing environmental impact [2,5,6]. BC can be produced through calcination, carbonisation via pyrolysis or gasification process. The produced BC mostly contains about 90% calcium phosphate in form of hydroxyapatite and 10% carbon [7]. Hence, as an adsorbent, BC contains a porous structure of hydroxyapatite with carbon distributed throughout it. Thus, the surface of BC is heterogeneity or homogeneous depending on the distribution of carbon on hydroxyapatite [8].

Unlike organic pollutants which can be degraded into harmless end products, metallic ions and anionic contaminants cannot be degraded. It has been proven that adsorption processes are cost-efficient and effective methods of removing metallic ions [9]. There have been promising results with BC as an effective and low-cost adsorbent for metal ions and anionic pollutants like fluoride and phosphorus removal [9–12]. There is a significant correlation between the physicochemical properties of the surface of the BC and the pH of the solution when it comes to adsorption capacity [13]. Aside from that, it is widely accepted that the thermal conditions used to produce BC, such as its temperature, residence time and atmosphere, can significantly influence its properties physicochemically [4,10]. An article published in 2019 reviewed the use of BC as a green sorbent for removing fluoride from drinking water [14]. However, the mechanism of metal ions and anionic element pollutants uptake during adsorption on BC has not been completely elucidated, prompting this review work. To predict the mechanisms of BC adsorbent for different contaminants, experimental data from the adsorption process must be modelled. Conversely, it is possible to improve the adsorption capacity of BC using suitable activation methods by modifying surface functional groups in a way that increases selectivity towards specific contaminants, or by acid/alkali treatment method that increases surface area, pore volume and provides a range of pore size distribution [14–16]. In spite of its lower surface area than activated (C), BC still contributes to high metal ions adsorption.

As an inorganic material, BC has high adsorption capacity and can efficiently remove metallic pollutants and other organic/inorganic elements or compounds from water [17,18]. The performance of a BC adsorbent, especially its porous network structure and surface chemistry, greatly influences the efficiency of the adsorption process. These physicochemical properties of BC are strongly influenced by synthesis conditions [1,10]. By optimising the pyrolysis conditions of bovine bone, a 143% increase in the metal uptake of the BC, ranging from 68.3 to 119.4 mg/g was achieved [10]. Based on the results, the pore size distribution rather than surface area determines the adsorption capacity. There is a need for porous materials capable of adsorbing mesoporous molecules. Finding an adsorbent that selectively adsorbs pollutants in this size range is a challenge. Mesopores control the adsorption process kinetics rather than micropores, which govern the amount of adsorbed contaminants. Additionally, adsorption is enhanced by the presence of surface functional groups. In a nutshell, adsorption is generally influenced by both the speciation of the adsorbate in solution (i.e. its different chemical forms) and the characteristics of the adsorbent (i.e. microstructural properties and surface chemistry). It has been found that, BC (82%) is the most effective adsorbent for the removal of fluoride ion compared to adsorbent from coal, wood, activated carbons obtained from coal, petroleum coke and wood, charcoals produced from *Q. mongolica, Q. pubescens, Q. phillyraeoides* and *C. obtuse* [19]. Waste bones derived BC and hydroxyapatite materials have been applied for removing the following contaminants *via* adsorption,

endotoxins [20], fluoride from drinking water [4,13,21,22], arsenic (V) [23–25], metallic ions such as Mn^{2+}, Fe^{2+}, Ni^{2+}, Cd^{2+}, Cu^{2+}, Zn^{2+}, Hg^{2+}, etc. from wastewater [10,26–28], phosphorous from wastewater [29,30], volatile organic compounds (VOCs) [31], separation *via* adsorption of ethanol, propanol, and butanol from aqueous solutions [32], removal of methylene blue from wastewater [33[34], and organic pollutant degradation [35]. BC is a low-cost adsorbent with large surface area and also a plausible support material for photocatalysts [33]. It is generally believed that adsorption is a result of electrostatic and non-electrostatic interactions between the adsorbate species and the surface of the bone char. In addition to BC adsorbent surface chemistry, specific pore size distributions of bone char contribute to selective adsorption by means of size exclusion, especially for cations contaminants. There are various mechanisms by which BC adsorbent surfaces can interact with pollutants molecules, including Van der Waals forces, hydrogen bonding, ion exchange, and electrostatic attraction [1,36].

From an environmental perspective, waste bone is converted into BC and used as an adsorbent to remove contaminants from wastewater or soil, thereby protecting the environment and offering waste management strategy. There are a number of parameters that affect BC's longevity and efficiency as an adsorbent, such as the initial contaminant concentration, the type of bone, the thermal method and conditions used for its production, and the removal capacity. This comprehensive review on the application of BC for purification and separation through adsorption captures the physicochemical properties of BC that makes its applicable as an adsorbent, the mechanisms of different contaminants adsorption onto the surface, the kinetic models of the removal rate, and the isotherm models for the equilibrium stage. Also, presented and discussed is different isotherm models used to describe adsorption data for bone derived adsorbents, which is a critical aspect in the design and control of adsorption process. Previously, a review on fluorine removal from drinking by BC has been reported [14], waste bone-to-materials and their application has been reported elsewhere [1], analysing and interpreting adsorption isotherms [37,38], and adsorption equilibria of metal ions on BC has also been reported in the literature [39]. Consequently, explanation of the physical meaning of the kinetic models and the methods for solving them, which is rarely discussed in the literature is covered in this study. This review, therefore, synthesises knowledge in the application BC for contaminant removal from water and soil, highlight new topic area for further research, presents the physical interpretations of kinetic and isotherm models used in BC adsorption studies, and discusses contemporary issues in adsorption.

2. Preparation and physicochemical characteristics of bone char

For the production of bone char, many types of bones can be used, such as those from camels, swine, ostriches, cows, chickens, goats, porcine, turkeys, and bovines [40,41]. These bones can be classified into two categories: hard bones (i.e. bovine, camel, etc.) and soft bones (i.e. fishbone, chicken, etc.). Gasification and pyrolysis are the two main methods of producing bone char (BC). A pyrolysis process is the thermal degradation of a waste bone under oxygen-limited atmosphere producing BC residue and bio-oil (250°C–850°C), whereas gasification involves the partial oxidation of bone biomass at high temperatures to produce a gaseous energy carrier (i.e. syngas) and BC. Unlike pyrolysis, gasification occurs at much higher temperatures, resulting in the production of gases. Pyrolysis produces BC with varying physiochemical characteristics that are influenced by various factors, including heat rate, gas atmosphere, and residence time [1]. Also, pyrolysis yields more BC than gasification. In contrast, calcination can be used to produce BC adsorbent, particularly hydroxyapatite material. Adsorption capacity and catalytic properties of BC are influenced by the surface properties and production conditions, including temperature and residence time. During BC synthesis, bone apatite minerals become dehydroxylated from its hydroxyapatite when high temperatures are applied. Residence time, heating rate, and purging gas are critical factors that affect the quality of BC produced at different thermochemical conversion temperatures [14].

The effect of pyrolysis temperature on produced BC: (a) yield and surface area, (b) pore volume and size, and (c) acid and basic sites are shown in Figure 1. The data used for this plots were obtained for devilfish BC produced through pyrolysis at

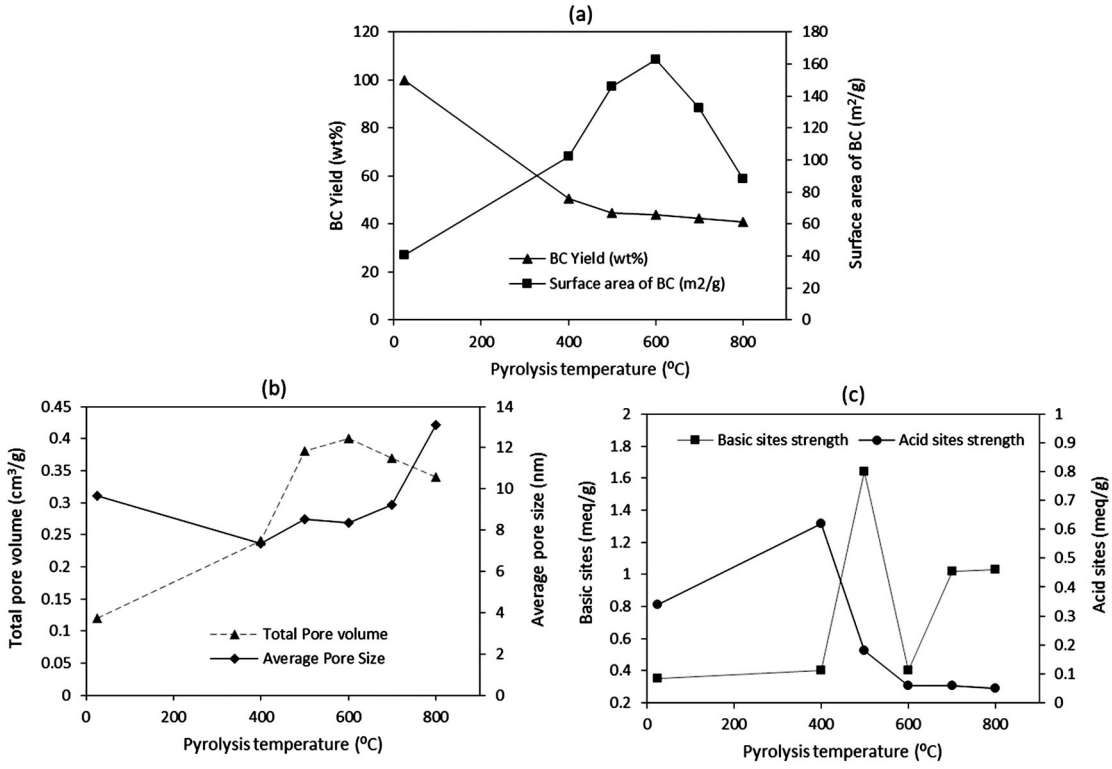

Figure 1. Effect of pyrolysis temperature on produced BC: (a) yield and surface area, (b) pore volume and size, and (c) acid and basic sites (Note, the plotted data was obtained from the article [42]).

temperatures range from 400°C to 800°C, and consequently used as an adsorbent for removal of fluoride from drinking water [42]. The result shows that the yield of BC decreases as the pyrolysis temperature increase, while the surface area increases to maximum at 600°C (163 m^2/g) before decreasing with further increase of pyrolysis temperature from 600°C to 800°C. It is worthy to note that the BC porous structure developed considerably as a result of pyrolysis. The total pore volume of the produced BC followed a similar trend with the surface area, whereas, the average pore diameter increases as the pyrolysis temperature increased. Hence, at temperatures of 600°C–800°C, BC's specific area and pore volume decreased due to dehydroxylation of its hydroxyapatite [14,42]. The increase in pore size from meso- to macro-pores resulting in the decrease in surface area as temperature increased beyond 600°C, suggests that about 5% of the total surface area is composed of macropores, while 95% is composed of mesopores and micropores [43]. It is believed that the pore structure and surface properties changes as a function of carbon content during charring [8]. Thus, the carbon content is a major determinant of BC adsorbent textural properties. It is well known that the functional groups such as hydroxyl on the BC surface develop electrical charges when exposed to an aqueous environment ($MOH \leftrightarrow M^+ + OH^-$ or $MOH \leftrightarrow M\bar{O} + H^+$, M denotes BC surface). When in suspension, the pH at which the net charge on the surface of BC is zero is called the point of zero charge (PZC). In the raw bone powder, the point of zero charge (pH_{PZC}) is 7.01, but as the pyrolysis temperature increases from 400°C to 800°C, it increases from 6.74 to 8.46 [42]. In BC adsorbents, PZC controls how easily pollutant ions are adsorbed. In spite of the fact that BC is an amphoteric material, the basic sites of BC were stronger than the acid sites (Figure 1c). The acid sites strength decreased as the pyrolysis temperature increased from 400°C to 800°C, while maximum basic sites strength was recorded at 500°C. BC adsorbent material with Ca/P less than or equal to 1.5 shows a higher acidity and low basicity, whereas Ca/P ratio greater than 1.67 shows a high basicity and lower acidity [2]. In addition to the Ca/P ratio, the acid and basic sites can be ascribed to evolution of hydroxyapatite formation and the decomposition of carbonate and other organic matter during pyrolysis. However, through protonation and deprotonation of the existing functional groups in BC, the

adsorbent surface charge can be controlled. These results demonstrate that the surface area, pore size distribution as well as acid and basic sites can be controlled through pyrolysis temperature. As a result of this analysis of the influence of synthesis conditions for preparing BC, the temperature at which bone wastes were pyrolysed would significantly affect the ability of the BC to adsorb pollutants. An analysis of the surface topology and morphology of BC revealed a solid phase with an irregular, compact and rough structure, with very few cavities [32]. This proves the heterogeneous nature of BC particles in terms of particle porosity, shape, and visible macropores, with the surface mainly composed of oxygen (50%), calcium (18%), carbon (17%), and phosphorus (12%), corresponding to carbon, calcium phosphate, and hydroxyapatite [22].

In spite of the fact that activated alumina showed superiority over BC breakthrough curves by approximately 200 bed volumes or 1.5 days, the BC adsorbent surface area had higher fluoride concentrations per square metre than activated alumina, which suggests that maximising BC surface area could improve adsorption [22]. The surface area of BC can be increased through pre-treatment with dilute acid/alkali and consequently optimised pyrolysis temperature. The main components of BC include hydroxyapatite [$Ca_{10}(PO_4)_6(OH)_2$], calcium carbonate [$CaCO_3$], calcium phosphate [$Ca_3(PO_4)_2$], and carbon [2]. BC exhibits a combination of micro-, meso-, and macroporosity, which makes it a good candidate for separation by adsorption and as a catalyst support. The properties of bone char are similar to those of activated C (non-polar adsorbent) and apatite (polar adsorbent) [17]. In other words, the mineral constituents within BC may influence both physicochemical properties and adsorption performance. But as a result of thermal sintering at high temperatures (>850°C), porosity and surface area could decrease.

In Figure 2, the nitrogen sorption isotherm of crushed cow bone and its BC as well as the pore size distribution (PSD) of fish BC are displayed. The adsorption–desorption hysteresis pattern indicates that both are type-IV isotherm, suggesting mesoporous structures. In bone char, the total gas uptake increased at a relative pressure below 0.5 (P/P_0), indicating that microporous pore structures were formed due to carbonisation (Figure 2a). It is obvious H3 hysteresis loop appeared in the range of $P/P_0 = 0.3–0.9$, confirming mesoporous material. Furthermore, the BC adsorbent shows a greater total gas uptake than raw crushed bone, which translates into more pores, increase pore volume and surface area. Hence, compared to crushed cow bone, which has a specific surface area of 0.96 m^2/g, a total porosity volume of 0.001 cm^3/g, and an average pore size of 6.49 nm, its char has 95.9 m^2/g, 0.236 cm^3/g, and 9.863 nm [44]. This suggests that charring of bone improves surface area and pore structure. Figure 2b shows that the PSD is dominated majorly mesopores followed by macropores and few micropores. BC contains a wide range of pore sizes (1.7–75 nm), with a predominant mesopore size distribution of 2 nm to 50 nm, as well as few micropores (<2 nm) or macropores larger than 50 nm [33]. Based on the classical Barrett–Joyner–Halenda (BJH) model adsorption cumulative distribution of pore size in BC, micropores accounted for 3.59%, mesopores accounted for 88.54%, and macropores accounted for 1.31%, suggesting a mesopore-dominated pore structure [45]. Despite the fact that micropores can offer the most adsorptive sites and dominate the adsorption capacity of adsorbents, macropores and mesopores also play an important role in adsorption. However, depending on the size of the pollutant, the diffusion resistance could increase if the micropore is too narrow, resulting in low diffusion rates. Since mesoporous structure is dominant in the BC, it makes intraparticle diffusion the most common rate-limiting step during the adsorption process. In comparison to untreated pork BC, the specific surface area increased by about 80% and porosity enhanced by acid treatment such as H_2SO_4 and H_3PO_4 [15]. Hence, acid or alkali can improve the porous structure and textural properties of BC, which is strongly to its applicability and adsorption capacity. It has been reported that the larger the specific surface area of BC, the more fluoride ions adsorbed [19]. Table 1 shows typical specific surface area, pore volume and pore size of BC derived from different bone sources. Studies have demonstrated BC to be low-cost adsorbents that have excellent ion-exchange characteristics, high adsorption capacities, mesoporous structure, and a large surface area in the range of 20–120 m^2/g depending on bone source.

By means of Fourier-transform infrared (FTIR) spectroscopy it was found that in addition to the main cation Ca^{2+}, BC consists of trace elements like

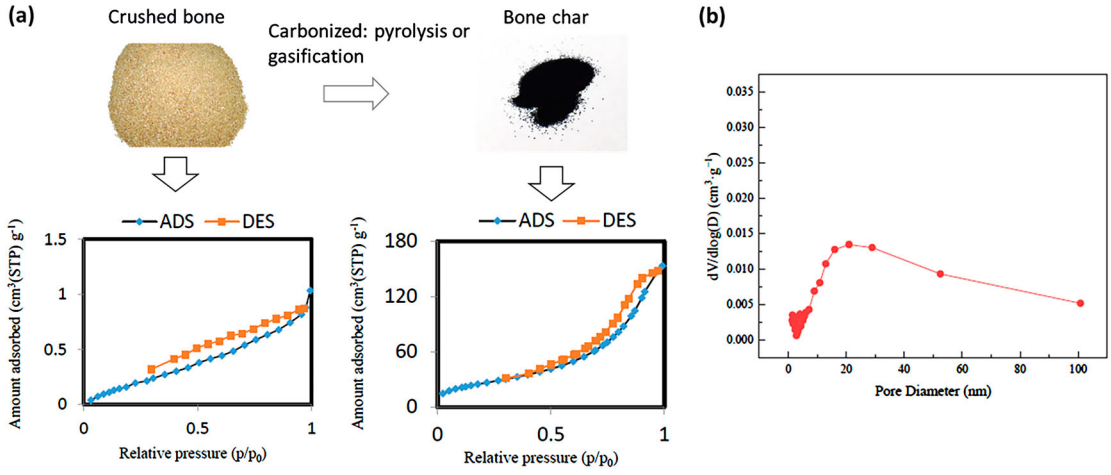

Figure 2. Textural characteristics: (a) Nitrogen sorption isotherm of crushed cow bone and its char [44] and (b) Fish bone char pore size distribution prepared at 600°C [46].

Na^+, Mg^{2+}, and K^+, and major functional groups, such as hydroxyl (OH^-), carbonate (CO_3^{2-}) and phosphate (PO_4^{2-}) in its structure [50,51]. Figure 3 shows the FTIR spectroscopy showing the functional groups in BC, as X-ray diffraction (XRD) of fishbone BC produced at pyrolysis temperatures of 300°C to 900°C as well as the ThermoGravimetric (TG) and Differential ThermoGravimetric (DTG) thermographs for raw cattle bone powder under a carbon dioxide atmosphere. The peaks associated with PO_4^{3-} functional group appeared at 1032, 962 and 563 cm^{-1} (Figure 3a), respectively [49]. The peak of the hydroxyl (OH^-) group occurred at 3443 cm^{-1}, whereas, the peaks at 1408 and 880 cm^{-1} represent the carbonate functional group (CO_3^{2-}). Therefore, in designing an efficient contaminants removal adsorbent from waste bone, surface properties and the conditions of BC production, such as temperature and residence time, seem to be crucial. This is because it has been reported that as pyrolysis temperatures rise above 700°C, the hydroxyapatite of BC is dehydroxylated, thereby decreasing its anionic pollutant such as fluoride adsorption capacity [4]. It has been reported that BC surface area, negative charge, and the number of oxygen-containing functional groups increased after hydrogen peroxide pre-treatment, despite a significant reduction in organic matter content [52].

The crystallinity of the BC increases as the pyrolysis temperature increased from 300°C to 900°C, evident in the intensity and sharpness diffraction peaks (Figure 3b). It can be observed in Figure 3b, that the diffraction peaks at 2θ values of 25.93°, 31.82°, 39.56°, 46.64°, 49.53°, and 53.23°, respectively, match the (002), (211), (130), (222), (213), and (004) diffraction peaks of hydroxyapatite powder (HAP). In addition, as pyrolysis temperature increases the conversion of bone powder into hydroxyapatite material increase. A higher surface oxygen-containing functional group was observed in BC samples with lower crystallinity, leading to a better adsorption capacity [52]. However, the TG and DTG shown in Figure 3c, describe the thermal response of raw bone powder to temperature during thermochemical process (e.g. pyrolysis) for BC production. The weight loss in the temperature range 20°C–200°C which is about 6.2 wt% can be credited to loss of adsorbed volatile molecules and moisture, thermal degradation of organic materials such as collagen, proteins, and fat tissue occurred in the temperature between 200 and 576°C with about 22.4 wt% weight loss and for temperatures ranging from 576°C to 880°C decomposition of carbonates and partial dehydroxylation process of

Table 1. Textural characteristics of bone chars (BCs) from different bone sources.

Parameter	Raw cattle bone [47]	Cattle BC [47]	Pig BC [48]	Fish BC [46]	Sheep BC [49]	Cow BC [44]
Ca/P	2.03	2.14	1.76		1.73	
Surface area (m^2/g)	0.461	50.3	87	19.3	34	95.91
Pore volume (cm^3/g)	0.004	0.305	0.15	0.047	0.16	0.237
Pore size (nm)	32.34	21.72	35	9.764	17	9.863

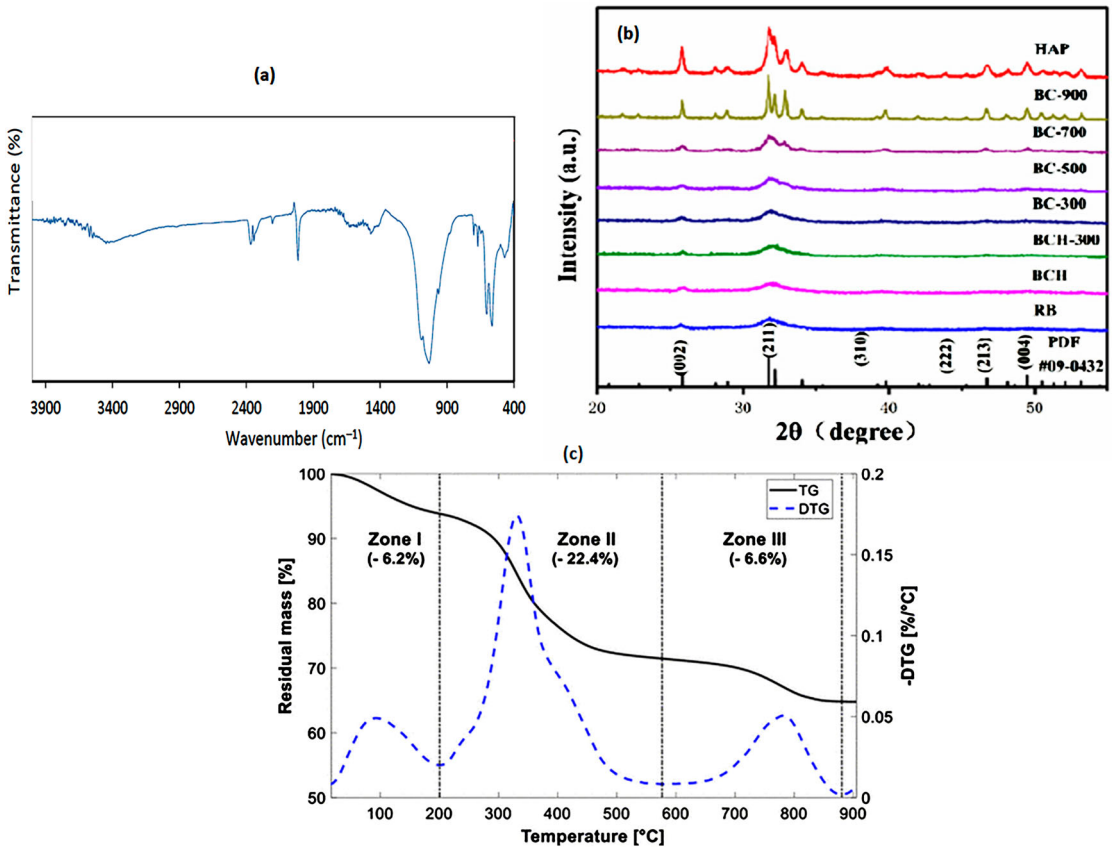

Figure 3. (a) FTIR spectra of bone char produced by pyrolysis of Sheep bone at 900°C [49], (b) XRD pattern for raw fishbone (RB), BCH (hydrogen peroxide treated bone powder), BCH-300 (hydrogen peroxide treated bone powder and pyrolysed at 300°C), BC-300 to BC-900 (BC produced at pyrolysis temperature 300°C–900°C) and hydroxyapatite powder, HAP, [52] and (c) ThermoGravimetric (TG) and Differential TG (DTG) plots for raw cattle bone powder under a carbon dioxide atmosphere [53].

hydroxyapatite happens, resulting in around 6.6 wt % weight loss [1,53]. In accordance with the total mass loss percentage with the TGA of about 35.2 wt%, the pyrolysis yield should be around 40%–62% depending on temperature. This explains the changes in the yields and textural properties of BC observed and reported in Figure 1. Hence, the thermal behaviour of waste bone powder will prove helpful in arriving at the optimum thermochemical temperature and atmosphere for BC production.

BC is a valuable adsorbent because its ability to exchange cations in aqueous solutions with a wide range of metal ions such as alkalis, alkaline earth metals, and transition metals [5]. Generally, the acidic sites are primarily attributed to PO–H from HPO_4^{2-} species (Brønsted sites) and Ca^{2+} cations (Lewis sites), whereas basic sites are accredited to surface functional groups PO_4^{3-} and OH^- (and perhaps other phases such as CaO, $Ca(OH)_2$, and $CaCO_3$) [1,5,6]. The strength of the acidic and basic sites reported in the literature was 0.29 and 0.62 meq/g for BC Fija Fluor [13], and 2.83 mmol/g (acidic site) and 0.51 mmol/g (basic site) for commercial BC [19], respectively. By protonating and deprotonating the hydroxyl groups on the surface of hydroxyapatite of the BC, basic and acid sites are formed [13]. The acid and basic sites distribution on the surface of a BC adsorbent is influenced by the Ca/P ratio. The BC adsorbent surface chemistry and specific pore size distributions play a role in selective adsorption. For instance, carbonate and hydroxyl in bone char is exchanged with fluoride ions during fluoride removal by BC. In other words, the surface functional groups of BC play a crucial role in regulating the adsorption capacity as well as its porous structure. In summary, the molecular interactions between a pollutant and BC depend on both the properties of the wastewater/solution (temperature, pH, and ionic strength/concentration) and the properties of the bone char itself (surface chemistry, surface charge, and textural properties). Therefore, BC adsorbent's main characteristic is its selectivity, which is

attributable to the variation in surface affinities for different contaminants, which enhances separation *via* adsorption.

3. BC adsorption mechanisms

Adsorption involves the mass transport of contaminants from a liquid phase to a solid phase adsorbent, which in this case is BC. The adsorption process consists primarily of four stages: (1) mass transfer of pollutants from the bulk of the solution to the exterior film surrounding of the adsorbent, (2) transport of pollutants across the external liquid film boundary layer to external surface sites, (3) through intra-particle diffusion, pollutants diffuse within the pores in the adsorbents, and (4) adsorption of pollutants on the adsorbent's internal surface [25,54]. The pollutant removal rate can be controlled by any of these processes. The final step is the interaction between contaminant and adsorbent, which an exchange process between the contaminant and the active sites of the adsorbent. It is, however, important to acknowledge that in a fully mixed batch system, mass transport from the bulk solution to the exterior surface is typically very fast, neglecting the transfer of contaminants from the bulk solution to the exterior film surrounding the adsorbent. In summary, the mass transport and adsorption on BC involves external mass transfer (film diffusion), internal diffusion (intra-particle diffusion) and adsorption on active sites, which is illustrated in Figure 4. In summary, adsorption process can be divided into three stages: (1) fast uptake of contaminants by the adsorbent, (2) gradual adsorption due to active adsorption sites on BC's surface, macropores, and mesopores, and (3) contaminant diffusion into micropores and achieving equilibrium adsorption. Therefore, the BC adsorbent abstracts one or more solutes in a solution or gas mix to its surface and holds them by intermolecular forces or bonds. There are two types of adsorption: physisorption and chemisorption, depending on the nature of the interaction between the pollutant and BC surface.

As a result of the physical and chemical interactions between pollutants and the BC adsorbent, adsorption of pollutants is a complex process [56]. Understanding the pollutant removal mechanisms is important for research and improving BC adsorbent's performance. The surface charge of BC is caused by the interactions between the surface functional groups and the ions present in the solution [13]. Therefore, an important factor in explaining the adsorption of ions on BC is the surface charge that depends on the type of ions present in solution, the surface properties, and the pH of the solution [1]. The Van der Waals force, hydrogen bonding, ion exchange, and electrostatic attraction are all mechanisms that BC adsorbent surfaces can use to interact with contaminants molecules in wastewater [36]. In fact, surfaces of hydroxyapatite (HA) in BC contain P-OH functional groups that act as sorption sites [57]. However, the mechanism of sorption postulated for metal ions is ion-exchange with Ca^{2+} ions in the hydroxyapatite component of BC [58]. Deydier et al. [59] reported that metal ions binding to HA derived from WABs comprises three successive steps, which are surface complexation and calcium hydroxyapatite of metal ions, $Ca_{10}(PO_4)_6(OH)_2$ dissolution and then precipitation of slow metal diffusion/substitution of Ca. Hence, dissolution/precipitation produces first a solid solution (Ca/MHA) until all the Ca in the BC has been substituted by the metal ions M. It was found that ion exchange of lattice Ca with Cd in aqueous solution, surface complexation between oxygen-containing groups, and electrostatic interactions between the positively charged Cd^{2+} and the negatively charged BC surface and oxygen-containing functional groups (e.g. $CaOH_2^+$ or POH_2^+) formed as a result of oxidation of organic matter were responsible for the adsorption and removal of Cd^{2+} by fishbone BC [52]. Also, it has been proven that metal ions adsorption onto BC adsorbent is dependent on the size of the ions and the BC pore size distribution [26]. Metal ions are adsorbed more closely and strongly with a smaller ionic radius and a greater valence. The ion exchange mechanism with Ca^{2+} depends on the functional groups of BC and also the metal ion sizes. In contrast, the higher the hydration of an ion, the farther it is from BC adsorption surface, and the weaker its affinity [39].

The removal of F^- ion by BC adsorption was due to ion-exchange with OH^- functional group in the structure to form the fluorapatite ($Ca_{10}(PO_4)_6F_2$), which is enhanced by the large surface area and pore volume [14]. As part of the ion exchange process, anions on the surface of the BC adsorbent are replaced with fluoride ions in liquid solutions. The anions on the BC adsorbent surface can be replaced with fluoride ions include OH^- and CO_3^{2-} [56]. But the

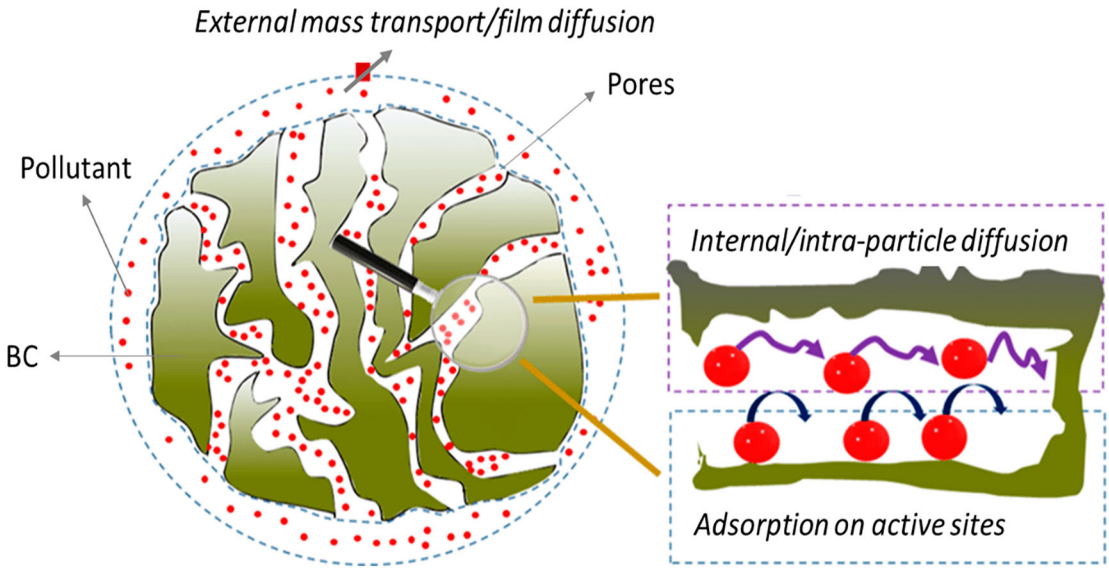

Figure 4. Illustration of diffusion steps of pollutant from liquid to solid adsorption [55].

ion exchange between OH^- and F^- is most reported mechanism of removal. This affirms the observation reported in the article by Abe and co-workers [19], that fluoride ions adsorbed onto BC are chemical in nature, since the amount of fluoride ions adsorbed increases with increasing temperature and decreasing pH. Recently, a similar observation was reported by Cruz-Briano and colleagues [42]. As a result, the adsorption of fluoride ion onto BC is endothermic. Similarly, the electrostatic interactions between the BC surface and the F^- ions play a crucial role in the removal process depending on the pH induced surface charges (positively charged surface will increase affinity for F^-) [13]. Electrostatic interaction, however, is strictly associated to the BC's surface charge, which is influenced by BC adsorbent's point of zero charge (pH_{PZC}) and solution pH value. The BC adsorbent becomes protonated and positively charged when the pH value falls below its PZC, and the deprotonated and negatively charged when pH is above PZC. In a nutshell, electrostatic charges transmitted by ionised pollutant molecules are influenced by the pH of the medium. Considering that BC has both basic and acidic sites, it would be charged when placed in an aqueous solution, allowing the ions to interact with the surface functional groups. On the other hand, methylene blue removal by BC decreased with increasing temperature, indicating that the adsorption process is exothermic [33]. This process involves cationic/anionic contaminants attracted to BC surface charges (–/+ve charges), leading to their adsorption. It has been reported that the presence of chloride ion increased the rate of fluoride ion uptake by BC, which was investigated by adding sodium chloride into solution to analyse the effects of another anion on the adsorption of the fluoride ion onto BC [19]. Thus, BC with acidic pH would support the adsorption of anions. However, dehydroxylation of the hydroxyapatite component influences ligand exchange in the BC adsorption mechanism [60]. This suggests that the adsorption of fluoride on BC occurs mostly due to electrostatic interactions between positively charged sites and fluoride ions, but chemisorption can also occur. As determined from X-ray photoemission spectra (XPS), fluoride bonded to calcium to form fluorite (CaF_2), while hydroxyapatite resulted in fluorapatite ($Ca_{10}(PO_4)_6F_2$) [13,21]. Following equations can be used to describe fluoride's chemisorption on hydroxyapatite of BC [21]. Hence, Ca phosphate has been shown in the bones to perform two important functions: adsorption and/or ion exchange, as shown in the reaction Schemes in equations 1–3.

$$\equiv Ca_{10}(PO_4)_6(OH)_2 + 20F^- \rightarrow 10CaF_2 + 3PO_4^{3-} + 2OH^- \quad (1)$$

$$\equiv Ca_{10}(PO_4)_6(OH)_2 + 2F^- \rightarrow \equiv Ca_{10}(PO_4)_6F_2 + 2OH^- \quad (2)$$

$$\equiv Ca_{10}(PO_4)_6(OH)_2 + xM^{2+} \rightarrow \equiv M_xCa_{(10-x)}(PO_4)_6(OH)_2 + xCa^{2+} \quad (3)$$

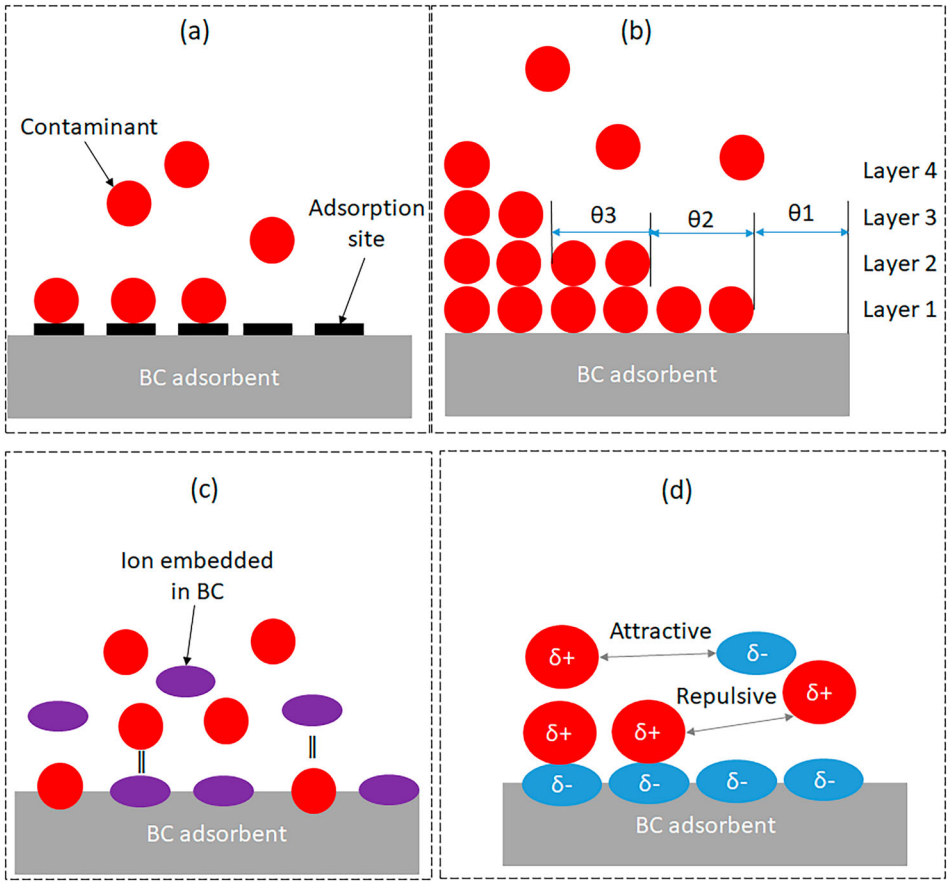

Figure 5. BC contaminant adsorption mechanisms: (a) mono-layer chemical adsorption, (b) multi-layer physical adsorption, (c) ion-exchange and (d) electrostatic interaction.

Based on this mechanism, metal ions (where; M^{2+} = Cd^{2+}, Mn^{2+}, Fe^{2+}, Co^{2+}, Ni^{2+}, Cu^{2+}, etc.) are adsorbed on the hydroxyapatite of BC surface via an ion exchange mechanism with Ca^{2+} ions leading to the formation of a new structure $[M_xCa_{(10-x)}(PO_4)_6(OH)_2]$, where x is the adsorbed heavy metal [10]. Adsorption of metal ions on BC surfaces may be enhanced by adjusting pH to induce electrostatic attraction between metal ions in wastewater and the charge on BC surfaces. Therefore, ion exchange and electrostatic attraction are key mechanisms responsible for metal ion adsorption on BC. The adsorption mechanism of various pollutants removal from wastewater or soil remediation using BC can be summarised as a combination two or more of these surface physiosorption and chemisorption, ionic exchange, adsorption and precipitation, electrostatic interaction, chemical complex, cation-π bonds, co-precipitation, and the formation of organo-metallic complexes and precipitates [7]. In Lewis acid–base interaction mechanism, bases donate pairs of electrons while acids accept, noting that metal ions are Lewis acids (e.g. Ca^{2+}) and anionic pollutants such as OH^-, F^- are Lewis bases. Based on this mechanism, the acids will react with bases to share electrons (removing the pollutant), resulting in no change in oxidation number. By protonation and deprotonation reactions occurring on the surface of BC, the adsorption sites of hydroxyapatite are formed that adsorb cations and anions pollutants [61,62]. Protonation of surface functional groups such as carbonate, phosphate, hydroxyl, etc. will take place at solution pH levels below the point of zero charge (pH_{PZC}) of BC [62]. This results in a positive surface charge on the BC. Thus, the BC having basic pH would favour the adsorption of positively charged pollutants and vice versa. Consequently, hydrogen bonds and π-π electron donor–acceptor interactions have been proposed as the mechanism between toluene and BC materials during adsorption for its

removal [31]. As a result of the functional groups and specific ligands on BC surfaces, a diversity of metals can interact with them to form their corresponding complex solid mineral phases. So, designing BC adsorbents and adsorption systems will require a thorough understanding of their adsorption mechanisms. Therefore, modelling the adsorption equilibrium data and characterisation of BC adsorbent before and after adsorption would be an excellent means of obtaining the adsorption mechanisms. The common BC adsorption mechanisms are summarised in Figure 5.

Among the adsorption mechanisms, chemical adsorption involves the formation of chemical bonds and monolayer of adsorbed molecules (i.e. there is no further adsorption at a site once an adsorbate molecule occupies it), physical adsorption involves van der Waals forces, multi-layers and interaction of adsorbed molecules, electrostatic interaction based on the electrical force between two (dis) similarly charged ions, and ion-exchange involves exchange of ionisable cations between the BC and the contaminant (Figure 5). Under the influence of van der Waals forces, contaminant molecules attach to the BC adsorbent surface in a process called physisorption. Dipole–dipole interactions are the main component of van der Waals forces. In electrostatic removal mechanisms, depending on the BC surface charge positively and negatively and the pH levels, the anionic functional groups in solution interact with the surfaces. Also, a significant role in the removal process is played by electrostatic interaction between the metal ions and BC surface depending on the medium pH. As the pH of the solution changes, the isoelectric point of the BC surface changes, which affects its electrical attraction to contaminant species [18]. Conversely, the exchange of cations presents on BC surfaces, in ion exchange mechanisms depend on the functional groups of BC as well as the metal ion sizes. Several transition metals and metallic ions pollutant possess a strong binding ability to these exchange sites. By modelling the equilibrium adsorption data with appropriate isotherm equation, analysing the BC adsorbent before and after adsorption, applying molecular dynamics, and calculating density functional theory (DFT), the adsorption mechanisms can be determined [18]. The most convenient and widely used method for modelling adsorption data is fitting of isotherm models.

4. Adsorption kinetics and isotherms modelling

4.1 Kinetic models

The kinetics of adsorption depicts the rate of contaminant uptake on the BC adsorbent. An adsorbent design and control depend heavily on understanding the dynamic behaviour of the adsorption system. In order to apply adsorption by BCs to industrial scales, it is imperative to study the rate at which pollutants are removed from aqueous solutions. Through the use of kinetic models, chemical reactions, diffusion control, and mass transfer mechanisms can all been explored during BC adsorption process [29]. To accurately evaluate contaminants' adsorption rates, kinetic models are essential. Adsorption processes are commonly analysed using experimental kinetic data to determine the effect of the external film boundary layer, internal diffusion resistance and adsorbent surface sorption.

The percentage removal (*%R*) of the contaminants by the BC can be calculated using equation (4). Whereas the amount of contaminant adsorbed per unit mass of the adsorbent, q_e (mg/g), can be estimated using equation 5.

$$\% R = \left(\frac{C_0 - C_e}{C_0}\right) \times 100 \tag{4}$$

$$q_e = \left(\frac{C_0 - C_e}{m}\right) V \text{ and } q_t = \left(\frac{C_0 - C_t}{m}\right) V \tag{5}$$

Where; C_0 denotes initial concentration of contaminant (ppm), C_e is the equilibrium concentration of contaminant (ppm), V is the volume of contaminant solution (L) and m is the mass of adsorbent (g).

The Ritchie rate equation (6) is defined when a number of surface sites of the adsorbent, n, are occupied by each contaminant. Form this generic equation, the Lagergren pseudo-first-order kinetic model and the second-order kinetic model can be predicted.

$$\frac{d\theta}{dt} = K_n(1 - \theta)^n \tag{6}$$

$$\text{For n} = 1;\ \ln(1 - \theta) = ln(1 - \theta_0) - K_1(t - t_0) \tag{7}$$

Where; $\theta = q_t/q_e$. q_e is the amount of the contaminants adsorbed at equilibrium per unit weight of the adsorbent (mg·g^{-1}); q_t is the amount of contaminants adsorbed at any time, t (mg·g^{-1}).

Table 2. Adsorption kinetic models.

Adsorption kinetic model	Equation	Remark
Intra-particle diffusion model	$q_t = k_p t^{0.5} + C$ q_t is plotted against $t^{0.5}$ to obtain a straight line, which does not necessarily pass through the origin. k_p denotes intra-particle diffusion rate constant (g/mg min) and the intercept of the plot, C, reflects the boundary layer effect or surface adsorption. The larger the intercept, the greater the contribution of the surface adsorption in the rate-limiting step. The resistance to film diffusion increases as the intercept increases. However, if intra-particle diffusion is rate-limited, then plots of pollutant uptake q_t vs. $t^{0.5}$ would result in a linear relationship.	1. The first step involves instantaneous adsorption or external surface adsorption. 2. In the second step, film/intra-particle diffusion controlled adsorption. 3. A slow adsorption rate occurs at the final equilibrium step, when the solute ions move slowly from large pores to micropores. 4. If the plot of pollutant uptake q_t vs. $t^{0.5}$ passes through the origin, then intra-particle diffusion is the sole rate-limiting step [63].
Elovich model	$\left(\frac{dq_t}{dt}\right) = a\ exp(-bq_t)$ or $q_t = \left(\frac{1}{b}\right) ln(ab) + \left(\frac{1}{b}\right) \ln(t)$ where a, b denotes constants of experimental data. The constant a can be regarded as the initial rate since $dq_t/dt \approx a$ as $q \approx 0$. Whereas, b is related to the extent of surface coverage and activation energy for chemisorption (g/mg). The assumption of $t >> t_0$ and validity of the model is checked by the linear plot of q_t vs. ln (t).	1. It is often used in adsorption kinetics to describe how chemicals adsorb (chemisorption) on adsorbent. 2. As the surface coverage increases, the chemisorption of pollutants on BC surfaces may decrease without any desorption of products. 3. System-compatible with heterogeneous surfaces for adsorption.
Ritchie model	$\left(\frac{q_e}{q_e - q_t}\right) = \alpha t + 1$ Note in most cases the intercept is slightly greater than 1. This is due to: (1) adsorption start time may not coincide with the time the pollution was adsorbed, or (2) the chemisorption occur rapidly initially on favour sites on the surface of the adsorbent.	1. This is an alternative to the Elovich equation for chemisorption of pollutant on n surface sites. 2. The rate of adsorption is dependent on the fraction of sites unoccupied at any time.

Prior to adsorption, the surface coverage of the adsorbent is assumed to be zero ($\theta_0 = 0$). However, adsorption that is preceded by diffusion through a boundary, when $\theta_0 = 0$ and $t_0 = 0$, the kinetics is then described by equation (8) for the pseudo-first-order equation first proposed by Lagergren in 1898.

$$\ln(1 - \theta) = -K_1 t$$
$$\ln(q_e - q_t) = \ln q_e - K_1 t \quad (8)$$

The Lagergren rate constant, K_1, is the slope of the plot of ln (q_e – q_t) against t (time) as shown in equation (8). Even if this plot is highly correlated with the experimentally obtained adsorption data, if the intercept does not equal the natural logarithm of the equilibrium adsorption of metal ions, the adsorption is unlikely to be first-order. In such occasion, the pseudo-second-order model mechanism given in equation (9) should be evaluated with the experimentally obtained adsorption data.

$$\frac{dq}{dt} = K_2(q_e - q_t)^2 \quad (9)$$

where, K_2 is the adsorption rate constant (mg·g^{-1}·min^{-1}). Upon integration with the boundary conditions; at $t = 0$, $q = 0$ and $t = t$, $q = q_t$, gives equation (10).

$$\frac{t}{q_t} = \frac{1}{h_0} + \frac{1}{q_e} t \quad (10)$$

Where; $h_0 = K_2 q_e^2$

h_0 is the initial adsorption rate. If the second-order kinetics is applicable, then the plot of t/q_t against t in equation (10) should give a linear relationship from which the constants q_e and h_0 can be determined. It also suggests several mechanisms are involved in the adsorption process. However, in these kinetic models, the adsorbed amount q_e changes with temperature (i.e. a thermodynamic equilibrium quantity), so the temperature dependence of the rate constant needs to be accounted for in the models. Hence, the activation energy can also be estimated with the Arrhenius equation and rate constants for various temperatures. Using the Arrhenius equation (11), the activation energy (E_a) and pre-exponential factor (A) of the adsorption process can be determined numerically. Other adsorption kinetics models used to study BC adsorption kinetic include Ritch-second-order, Elovich equation, and intra-particle diffusion model [63], as shown in Table 2.

$$\ln K_{ads} = lnA - \frac{E_a}{RT} \quad (11)$$

Where; K_{ads} denotes adsorption rate constant, T is temperature (K), and R constant. The plot of ln K_{ads}

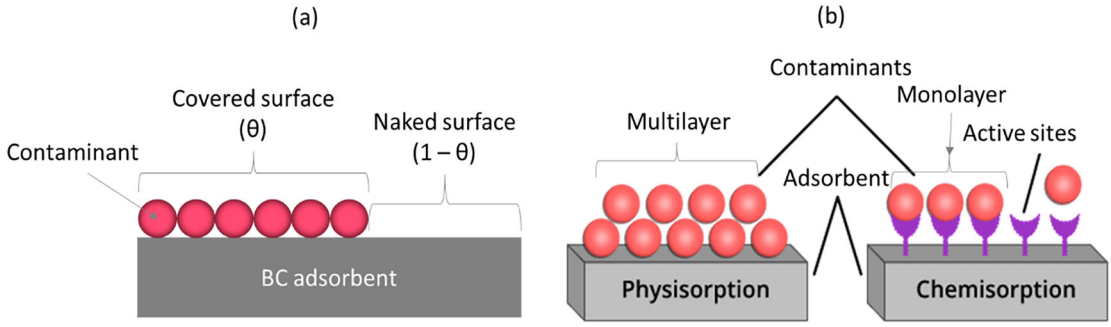

Figure 6. Adsorbent contaminant surface interaction: (a) surface coverage by contaminant adsorption and (b) physisorption and chemisorption.

versus 1/T is linear from which E_a and A would be determined.

There are, however, some issues with the application of pseudo-first-order as well as pseudo-second-order kinetic models. Firstly, both models lack specific physical meanings and are empirical models [64]. It is therefore challenging to establish the mass transport mechanisms by these empirical kinetic models. Several adsorption kinetic models, their physical meanings, applications, and methods of solving them were presented by Wang and Guo [64].

4.2. Isotherm models

An adsorption isotherm model describes the relationship between the equilibrium concentrations of contaminants in the liquid-phase and the equilibrium amount of adsorption in the solid-phase at a given temperature [18]. When adsorption and desorption processes reach equilibrium, this is called adsorption equilibrium. In a nutshell, the amount of adsorbed contaminants from the solution equals the amount of desorbed contaminants from the adsorbent. Adsorption isotherms can be used to establish the appropriate correlation for equilibrium curves to optimise sorption system design [25]. In general, equilibrium data are correlated using suitable theoretical or empirical isotherm models showing the solid-phase concentration plotted against the solution-phase concentration [65]. There are many mathematical forms of adsorption isotherm models, some based on simplified physical descriptions of adsorption and desorption, while others are empirical correlations.

The isotherm models of Langmuir and Freundlich were used to fit the experimental adsorption equilibrium data of pollutants on BC. According to the Langmuir model, adsorption takes place in homogeneous monolayers in which the adsorbate is attracted to all sites equally. In contrast, BC primarily contains carbon and hydroxyapatite distributed randomly on its surface, which violates Langmuir's assumption of homogeneity [39]. Whereas, Freundlich isotherm, adsorption occurs on heterogeneous surfaces of adsorbent as multilayer adsorption process. Based on Freundlich's isotherm model, the active sites and energy of a heterogeneous surface are distributed exponentially.

Figure 6 shows the interactions between adsorbent surface and contaminants. Generally, adsorption mechanisms include chemical adsorption which involves the formation of chemical bonds between the contaminant and adsorbent, physical adsorption due to van der Waals attraction, and ion exchange (Figure 6b). The adsorption data can be described by isotherm models, which are critical for designing an adsorption system. Furthermore, models of adsorption isotherms help predict the mechanisms of adsorption and estimate the maximum adsorption capacity, which is important in evaluating adsorbent performance. The adsorption equilibrium model commonly used is the Langmuir-Freundlich (Sips isotherm) equation 12, which assumes that the maximum adsorption occurs when a single layer of contaminant covers the surface [66]. Based on the assumption that the contaminant species occupy n sites of the adsorbent (Figure 6a), adsorption rate is proportional to naked surface (1−θ), while desorption rate is proportional to covered surface (θ). The rate

Table 3. Reported isotherm models relevant to BC adsorbents.

Adsorption isotherm models	Remarks
Freundlich Isotherm (linear form) $logq_e = logK_F + \frac{1}{n} logC_e$ K_F denotes adsorption capacity (L/mg), C_e the concentration of pollutant at equilibrium (mg/g), and $1/n$ is adsorption intensity, which provides information about the energy distribution and the heterogeneity of the adsorbent sites ($1/n$ can range from 0 to 1).	1. Adsorbents' surfaces are heterogeneous, and the distribution of active sites and their energies is exponential. 2. The Freundlich equation does not predict an adsorption maximum, which is one of its major limitations. Second, the equation has no theoretical basis, purely empirical one. 3. The Freundlich isotherm model is used to describe the adsorption of molecules arranged in multilayers with interaction between them.
Temkin Isotherm (linear form) $q_e = \frac{RT}{b} lnK_T + \frac{RT}{b} lnC_e$ b denotes Temkin constant relating to the heat of adsorption (J/mol), R gas constant, T temperature, and K_T is Temkin isotherm constant (L/g)	1. According to the Temkin isotherm model, adsorption heat decreases linearly with increasing adsorbent coverage. 2. Upon adsorption, binding energies are uniformly distributed up to a maximum. 3. Multilayer adsorption ignores extremely small and extremely large concentration values, but considers interactions between the adsorbent and the contaminant.
Langmuir isotherm (linear form) $\frac{C_e}{q_e} = \frac{1}{K_L q_m} + \frac{C_e}{q_m}$ q_m denotes the maximum monolayer adsorption capacity (mol/g), K_L the Langmuir constant (L/mol), and q_e and C_e are the adsorption capacity (mol/g) and equilibrium concentration (mol/L). This model converts to Henry's model at very low concentrations ($K_L C_e \ll 1$).	1. The Langmuir isotherm model assumes that adsorption occurs at homogeneous sites within an adsorbent (i.e. all sites are equal, resulting in equal adsorption energies). 2. Adsorption proportional to the fraction of adsorbent surface which is expose, while desorption occurs as a function of the fraction of adsorbent surface which is covered by pollutants. 3. Pollutants adhere to a specific site on the surface of the adsorbent, forming a single-layer/monolayer. 4. Adsorption occurs at constant energy, and pollutant molecules do not migrate or interact on the surface.
Redlich-Peterson (R-*P*) isotherm (linear form) $ln\left(K_R \frac{C_e}{q_e} - 1\right) = ln(a_R) + \beta\, ln(C_e)$ K_R denotes R-*P* constant (L/g), a_R the R-*P* constant (L/mg) and β the exponent which is the slope of the plot, value between 0 and 1.	1. It includes both the features of Langmuir and Freundlich isotherms to form an empirical adsorption isotherm of three parameters. 2. Its versatility allows it to be used in either homogeneous or heterogeneous systems. 3. Unlike ideal monolayer adsorption, the adsorption mechanism is mixed.

equation can be derived by merging the forward adsorption rate step and the reverse desorption step as follows.

$$\frac{d\theta}{dt} = k_{ad} C(1-\theta)^n - k_d \theta^n \tag{12}$$

When the adsorption attains equilibrium (i.e. $d\theta/dt = 0$), resulting in the Langmuir-Freundlich equation 13 (Sips Isotherm).

$$q_e = \frac{K_{LF} C_e^{1/n}}{1 + a_{LF} C_e^{1/n}} \tag{13}$$

The Redlich-Peterson and Sips adsorption isotherm models combine Langmuir and Freundlich models with three parameters. The parameters of the Sips isotherm model (equation 13) are controlled by temperature, pH, and change in concentration. Sips isotherm model follows Freundlich isotherms at low contaminant concentrations. At high concentrations, it exhibits the monolayer adsorption behaviour of the Langmuir model. Adsorption isotherm models must be fitted with experimental adsorption data to understand and predict adsorption behaviour. However, the difference between the Sips and the Langmuir isotherm equations is the heterogeneity factor n, generally less than 1 and when n is equal 1, the surface is homogeneous (Langmuir isotherm). This parameter, therefore, indicates how heterogeneous an adsorbent surface is based on its value, the smaller values are more heterogeneous. Based on the most widely used adsorption isotherm models, Table 3 summarises some isotherm models applicable to BC adsorbents for the removal of contaminants from wastewater. It is clear that Langmuir isotherm model described the equilibrium data for cations contaminants, while Freundlich isotherm model for anions such as fluoride and phosphate. This evidence demonstrated that the adsorption process of fluoride, phosphate and toluene was not just simple mono-layer adsorption, unlike metal ions which are mostly single-layer adsorption. Also, the pseudo-second-order rate equation describe the kinetics of metal ions adsorption on BC. To develop the specific model that describes experimental data regarding adsorption, Lagergren and Langmuir kinetic models are used as the basis. The Langmuir equation applies to adsorption with less than monolayer coverage, making it more suitable for chemisorption studies since it only involves monolayer coverage (i.e. only one molecule can be adsorbed at each site (Figure 5b)) and constant adsorption

Table 4. BC adsorption kinetic equation and isotherm models for some pollutants and different bone sources.

BC source	Pollutants	Kinetic and isotherm model	Remark	Reference
Cow bone	Mn^{2+}, Fe^{2+}, Ni^{2+} and Cu^{2+}	Pseudo-second-order rate equation and Langmuir fit.	1. Due to size and pH conditions, Cu^{2+} adsorb the most on cow BC. 2. Adsorption capacity depends on pH.	[26]
Cow bone	As(V)	Pseudo-second-order kinetic and Langmuir models fit.	1. The adsorption capacity is a function of flow rate, bed height and adsorption cycle times. 2. The transport behaviour of As(V) in BC can be modelled by convection dispersion equation.	[24]
Cattle bones	F^-	Freundlich isotherm model fit.	1. A pH decrease from 12 to 3 dramatically increased the adsorption capacity of BC. 2. BC has a fluoride adsorption capacity that is 1.3 times lower compared to IRA-410 polymeric resin and 2.8 times greater compared to Alcoa F-1 activated alumina.	[13,21]
Camel bone	Hg(II)	Langmuir isotherm model fit.	1. The adsorption capacity was 28.24 mgHg(II)/g BC. 2. pH 2, contact time 30 min, and temperature 25°C are the best conditions for Hg removal.	[27]
Swine bone	Co^{2+}	Pseudo-second-order kinetic and Freundlich models fit.	Based on batch kinetics, a rapid uptake was observed during the first five minutes, followed by a slow diffusion process within the particles.	[69]
Fish bone	Cd^{2+}	Pseudo-second order kinetics model and the Langmuir model fit.	Based on the adsorption results, it appears that chemical adsorption controls the adsorption rate, and that monolayer adsorption is the dominant one.	[46]
Cow	F^-	Freundlich isotherm slightly better than Langmuir model fit.	Fluoride sorption capacity was unaffected by the presence of chloride, sulfate, and nitrate ions in solution, the presence of carbonate or bicarbonate ions negatively affected it.	[67]
Sheep bone	*P*	Pseudo second-order kinetic and Freundlich isotherm models fit.	1. BC was effective in removing phosphate from aqueous solutions, especially at concentrations between 2 and 100 mg/L. 2. The optimum pH is 4, and higher pH decreased the adsorption rate significantly. As temperature increases from 20°C to 40°C sorption capacity increase, illustrating endothermic adsorption.	[29]
Bovine bone	Zn^{2+}, Cd^{2+}, and Ni^{2+}	Pseudo-second order kinetic equation and Sips isotherm model fit.	1. The removal performance followed the trend $Cd^{2+} > Zn^{2+} > Ni^{2+}$. 2. The ion-exchange between the calcium, from the hydroxyapatite structure of BC, and the metal ions in solution played an important role in the adsorption process.	[10]
Bovine bone	Volatile organic compounds (VOCs)	Pseudo second-order kinetic and Freundlich isotherm models fit.	As a result of the modification of H_3PO_4, there was an effective acceleration of the adsorption process after activation of K_2CO_3.	[31]

energy. Also, a molecule/contaminant that is adsorbed does not interact with another. However, physical adsorption does not only occur on monolayers, but can also occur on subsequent layers (Figure 5b). Thus, molecular interactions are possible due to the multilayered structure of adsorbed molecules/contaminants. As a result, several other adsorption isotherm models have been developed, detailed reviews of adsorption isotherm models have been reported in the literature review by Ayawei and co-workers [37] and also in recent times by Wang and Guo [18].

The Langmuir isotherm model has been used to describe the removal of metal ions from solution via BC [10,26], while the Freundlich isotherm model for fluoride, toluene and phosphate removal [13,29,31]. find the adsorption mechanism and the best fit model, all adsorption models should be applied to the contaminant adsorption on BC data set. Some of these isotherm models, such as Freundlich, Sips, Temkin, are empirical models without substantial theoretical support. Optimum isotherms are those that best fit the experimental data, with high coefficients of determination (R^2) or low values of other statistical parameters, such as nonlinear chi-squares (χ^2) and residual sums of squares errors (SSE).

Recently, Yang and co-workers [46], found that by modifying fish BC by chitosan-Fe_3O_4, the saturated adsorption capacity achieved for the chitosan-Fe_3O_4-BC to Cd(II) was 64.31 mg/g, which was 1.7 times than unmodified BC. This suggests that modifying BC with an appropriate dopant, the adsorption capacity and affinity can be enhanced significantly. This is consistent with previous study reported by Nigri and colleagues [67], they found that acid treatment and Al-doped cow BC exhibited highest sorption capacities for fluoride than their unmodified counterparts. The summary of variant contaminants, kinetic and isotherm models used to describe adsorption data by different BC source is shown in Table 4. Consequently, Langmuir and Elovich models accurately described experimental data of Remazol brilliant blue R (RBBR) adsorption onto BC, showing monolayer adsorption on homogeneous surfaces

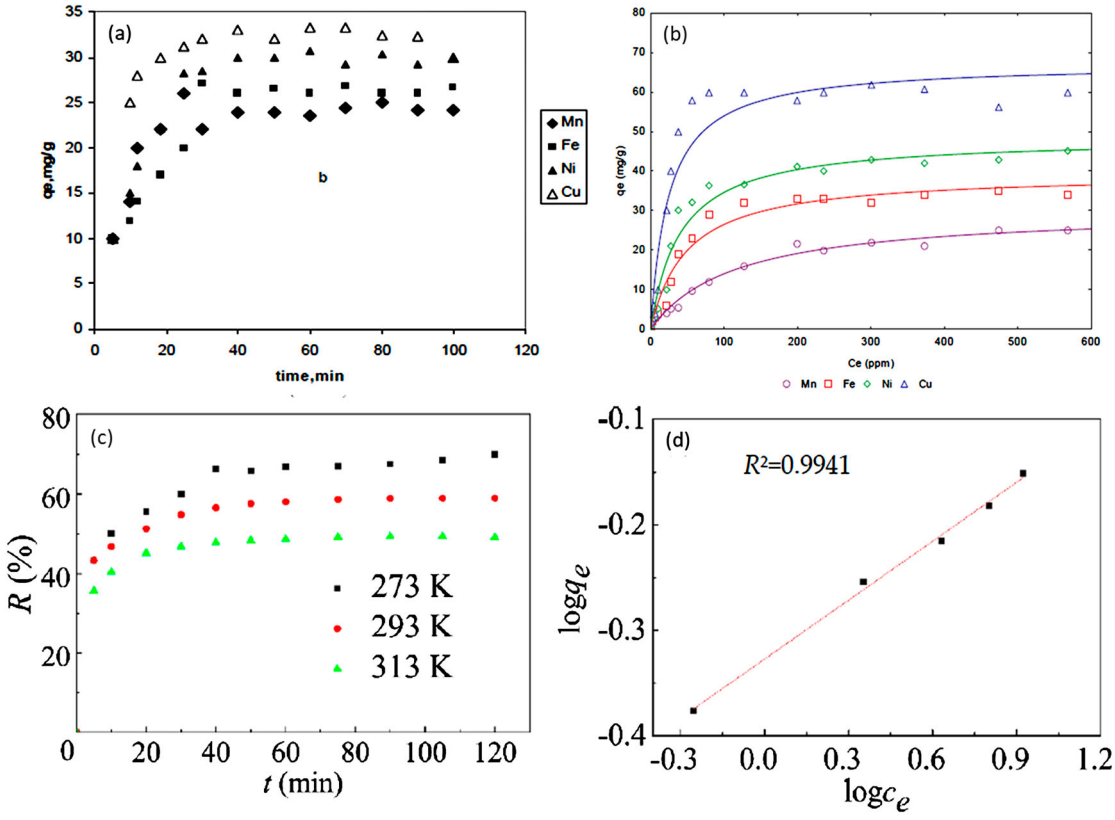

Figure 7. (a) Cow bone BC for removal of Mn^{2+}, Fe^{2+}, Ni^{2+}, and Cu^{2+} as a function contact time at C0 20 mg/L, BC dose 0.02 g, pH 5.1 and temperature, 298 K, (b) Langmuir isotherm model for the adsorption of Mn^{2+}, Fe^{2+}, Ni^{2+}, and Cu^{2+} cations [26], (c) Bovine bone BC removal of methylene blue from aqueous solution as a function of adsorption temperature on methylene blue adsorption and (d) Freundlich isotherm model for the adsorption of methylene blue [33].

(20.6 mg/g) with chemisorption [68]. In a study of cobalt sorption onto BC, the Freundlich isotherm model proved to be an accurate description of the equilibrium adsorption data [69]. It was found that ion exchange with Ca^{2+} in the hydroxyapatite of the BC is the main mechanism of Co^{2+} removal and multilayer coverage on the heterogeneous surface.

In another study, an ox BC was activated and functionalised with magnetite nanoparticles to remove reactive 5G blue dye *via* adsorption [70]. It was found that the functionalised BC adsorbent followed pseudo-first-order kinetics, with equilibrium experimental data fitting better to the Langmuir model, with q_{max} of 91.58 mg/g controlled by both intraparticle diffusion and surface diffusion. Furthermore, a bone char (surface area 114.15 m^2/g) produced *via* pyrolysis of cattle bones which was surface treated with acetone was investigated for the adsorption of 17β-estradiol from aqueous solutions [71]. The result showed that the maximum adsorption capacity of 17β-estradiol on BC was 10.12 mg/g and uptake can be predicted by the pseudo second order kinetic equation, while intraparticle diffusion was the rate limiting step. Both Langmuir and Freundlich isotherm models fitted the experimental adsorption equilibrium data. With the help of an ethanol–water solution, the saturated BC was regenerated and adsorption capacity was restored to 85% of its initial capacity in the third cycle. Using a batch agitation system, Cu(II) and Zn (II) ions sorption were studied on BC (surface area 100 m^2/g and pore volume 0.225 cm^3/g) around pH 5 [72]. The uptake mechanisms are by means of adsorption and ion exchange (the chemical formula after ion exchange is $Ca_{10-x}M_x(PO_4)_6(OH)_2$, where M denotes the divalent metal ions Cu^{2+} or Zn^{2+}) from the solutions. It was shown that the metal ions sorption rates are primarily controlled by pore diffusion, and a numerical film-pore diffusion model was developed to describe this process. In the study, Langmuir's model and a film-pore diffusion mass transport model were used to correlate experimental data from adsorption isotherms and batch kinetics. There was an excellent

correlation between the theoretical model and the experimental data.

The BC adsorbent material is an environmentally friendly, non-toxic, affordable, and straightforward alternative to chemically synthesised or modified adsorbent materials. BC uses its distinctive and abundant ionic polarity sites such as Ca^{2+}, PO_4^{3-}, CO_3^{2-}, OH^-, etc. to adsorb pollutants. Using cationic Malachite Green (MG) dye and anionic Sunset Yellow (SY) dye, Li et al. [73] investigated the adsorption and desorption behaviours of bovine rib BC. According to the results, MG adsorption increases as pH increases, but SY adsorption decreases with pH, with optimum pH values of 7 and 3, respectively. It was established that the adsorption mechanism of ionic dyes on BC is mainly determined by the interactions between pore filling, electrostatic interaction, chemical bond formation, and ion exchange. Recently, the application of calf BC to remove humic acid from water was reported [74]. According to the results, prepared calf BC with a surface area of 112 m^2/g shows an adsorption capacity of 38.08 mg/g (HA = 20 mg/L, pH = 4.0). Data from the adsorption experiment fit well with the pseudo-second-order model and Langmuir isotherm showing that monolayers are formed during adsorption. To recycle the humic acid saturated calf BC, a significant regeneration was achieved with the aid of NaOH treatment. Since BC can be regarded as an adsorbent with a complex chemical structure constituted of 9%–11% of amorphous carbon-phase, 7%–9% of calcite and 70%–76% of hydroxyapatite (i.e. $Ca_{10}(PO_4)_6(OH)_2$), it could be anticipated that the functional groups of both organic and inorganic phases may well interact with pollutants [60]. BC prepared by pyrolysis was evaluated for the adsorption of toxic dental clinic pollutants such as fluoride, mercury and arsenic as the target pollutants [60]. It was found that the degree of hydroxyapatite dehydroxylation affected the adsorption mechanism through ligand exchanges involved in the removal of these pollutants by BC. Adsorption of fluoride and mercury on the surface of the BC was observed to be an endothermic multimolecular process, while that of arsenic on was monolayer interaction with the adsorption sites. Results showed that dehydroxylation of hydroxyapatite and decomposition of BC carbonates resulted in a significant reduction of the metal ions uptake of this adsorbent at carbonisation temperatures greater than 700°C. In metal ions adsorption with BC, metal–oxygen interactions from hydroxyapatite play a relevant role in an ion-exchange process. For understanding the adsorption mechanism in a BC system and predicting its behaviour, the experimental adsorption data must be fitted with the appropriate adsorption isotherm model. In recent time, nitrogen-functionalised BC was synthesised using pristine bone char and ammonia hydroxide for surface modification [46] The nitrogen-functionalised BC was applied to study the adsorption of multiple aquatic pollutants such as representative heavy metal Cr(VI), nuclide U(VI), and methylene blue. The results showed that nitrogen-functionalised BC exhibited excellent maximum adsorption capacities for heavy metal Cr(VI) (339.8 mg/g), nuclide U(VI) (466.5 mg/g), and methylene blue (338.3 mg/g) at pH 5.0 and temperature 293 K, demonstrating a significant potential in the adsorption of multiple types of pollutants. Analysing multiple spectroscopic technologies, it was discovered that electrostatic attraction, surface complexation, precipitation, cation exchange, and cation-π and π–π interactions are the main adsorption mechanisms. As a result, the functionalization of BCs will enhance their performance and multifunctionality in removing pollutants.

Figure 7 shows typical adsorption data and isotherm models for metal ions and methylene blue. The uptake of metal ions increases with time, reaches a maximum after 20 min and equilibrated in 60 min. However, the order of affinity for BC and adsorption can be summarised as thus: $Cu^{2+} > Ni^{2+} > Fe^{2+} > Mn^{2+}$. The reported amounts adsorbed at equilibrium (q_e) by the BC are as follows: 29.56 mg/g (Mn^{2+}), 31.43 mg/g (Fe^{2+}), 32.54 mg/g (Ni^{2+}) and 35.44 mg/g (Cu^{2+}) [26]. This can be attributed to the size of the cations and the pore size distribution within the BC in addition to the ion exchange mechanism taking place. The maximum removal in terms of percentage was between 75% and 98% from Mn to Cu. As the hydrated ionic size decreases, metal ions are easily adsorbed (i.e. $Cu^{2+} < Ni^{2+} < Fe^{2+} < Mn^{2+}$). This is because as the ionic size becomes smaller, the metal ion diffuses easily into the micropores of the BC. The pseudo-second-order kinetic equation and Langmuir isotherm model (R^2 range from 0.9987 to 0.9999) describe better the BC experimental adsorption data for these metal ions. In other words, the plateau values seen in Figure 7b represent monolayer coverage on the surface of the BC.

Thus, carbon is well distributed throughout the porous hydroxyapatite structure as a uniform thin layer on the BC. Consequently, during the first few minutes (10 min), methylene blue rapidly adsorbs on BC, but from macropores to micropores, the diffusion path decreases within the narrow pore size during the second stage of slow adsorption.

It is evident from the plot of q vs. $t^{0.5}$ of the intraparticle diffusion model for intraparticle region, showed that methylene blue adsorption does not pass through the origin, implying the rate-limiting step is a combination of intraparticle diffusion and the boundary layer effect due to external diffusion from bulk solution to the BC surface [33]. Since BC has a predominantly mesoporous structure, intraparticle diffusion was be the rate-limiting step during adsorption methylene blue. The results show that the pseudo-second-order kinetic model and Freundlich. This is expected as the BC surface is highly heterogeneous, the adsorption isotherm demonstrates a multi-layer adsorption methylene blue. Changing adsorption temperatures from 273 to 313 K results in a decrease in methylene blue, which suggests an exothermic process. However, sodium hydroxide can be used to regenerate BC [22].

5. Error analysis between experimental data and isotherm model

The optimal analysis of adsorption data requires error functions. By minimising the difference between experimental data points and the predictions of the model equations, the parameters of the kinetic and isotherm models can be determined. According to studies, linearising adsorption isotherms usually changes the error structure of adsorption data [75]. When nonlinear equations are transformed into linear forms, their error structure is altered, and the standard least-squares assumptions of error variance and normality are violated. In the case of an isotherm equations with three or more parameters, a simple linear analysis cannot be performed. Therefore, nonlinear optimisation has been found to be the most effective method for arriving at the best isotherm equation [76,77]. Hence, the purpose of nonlinear regression is to minimise (or maximise) the error between adsorption data and predicted isotherms using convergence criteria as an alternative to linear regression. The error analysis involves the application of statistical methods to evaluate the difference between experimental data and the isotherm predicted values. By comparing the squared errors, the best-fit isotherm model can be identified, which is the model that produces the minimal error. One of the objective functions used in the minimisation scheme has been the sum of the errors squared (SSE). The square of the errors increases as the concentration in the liquid phase increases, which is one of the bottlenecks of SSE function. So, a better fit is observed at high concentration. Others include Root Mean Square Error (RMSE), Hybrid fractional error function (HYBRID), Average Relative error (ARE), Marquardt's percent standard deviation (MPSD), Nonlinear chi-square test (χ) and Coefficient of determination (R^2).

$$SSE = \sum_{i=1}^{N} (q_{Exp,i} - q_{Cal,i})^2$$

where q_{Exp} denotes the experimental adsorption capacity data, q_{Cal} the theoretical adsorption kinetic/isotherm model and N number of data points.

$$MSE = \sqrt{\frac{1}{N}\sum_{i=1}^{N} (q_{Exp,i} - q_{Cal,i})^2}$$

Hybrid fractional error function (HYBRID) was developed in order to improve the sum of the squares of the errors at lower liquid-phase concentrations. It therefore improves the fit at low concentration values compare to SSE method. The method includes number of degrees of freedom, which is $N - P$ as a divisor.

$$\text{HYBRID} = \frac{1}{N-P}\sum_{i=1}^{N}\left[\frac{(q_{Exp} - q_{Cal})^2}{q_{Exp}}\right]_i$$

This function includes the number of data points (N), minus the number of parameters (P) in isotherm equation.

In the average relative error (ARE) formula, the fractional error distribution across all independent variables is minimised:

$$\text{ARE} = \frac{100}{N}\sum_{i=1}^{N}\left|\frac{q_{Cal} - q_{Exp}}{q_{Exp}}\right|_i$$

Marquardt's percent standard deviation (MPSD):

$$\mathrm{MPSD} = 100\sqrt{\frac{1}{N-P}\sum_{i=1}^{N}\left(\frac{q_{Exp}-q_{Cal}}{q_{Exp}}\right)^2}$$

Nonlinear chi-square test (χ):

$$\chi^2 = \sum_{i=1}^{N}\frac{(q_{Exp}-q_{Cal})^2}{q_{Exp}}$$

The coefficient of determination (R^2), the best fit is the isotherm model which R^2 is close to or approximately 1.

$$R^2 = \frac{\sum(q_{Exp}-\bar{q}_{Cal})^2}{\sum(q_{Exp}-\bar{q}_{Cal})^2+\sum(q_{Exp}-q_{Cal})^2}$$

q_{Exp} denotes measured experimental ion concentration; q_{cal} the calculated ion concentration with isother models; N the number of experimental data points; and P the number of parameters in each isotherm model.

The isotherm parameters are likely to be different for each error function. Hence, the choice of error function can affect the derived isotherm parameters. The parameters of the isotherm models can be obtained by minimising the error functions. The minimisation of the difference between experimental measurements and the model calculated values can be performed using the solver add-in within Microsoft Excel, Python software, MATLAB or any other suitable data analysis software. In order to obtain the parameters involved in the isotherms, as well as the optimum isotherm, non-linear regression was found to be a more effective method than linear regression [77]. MPSD was found to be the best error function in minimising the error distribution between experimental equilibrium data and predicted isotherms for two parameter isotherms, whereas R^2 was found to be the best error function for three parameter isotherms for the sorption of basic red 9 by activated carbon. As well as the size of the error function, experimental data should also be used to authenticate the theory behind the predicted isotherm.

6. Performance of BC in a packed-bed column

BC adsorption studies tend to be limited to batch studies or equilibrium experiments, which may make it difficult to extend these works to large-scale applications. In contrast to batch system, there are several advantages to using a packed-bed column adsorption system, including the ability to contact the BC adsorbent effectively with the fluid to be treated, the ability to treat large volumes in a short period of time (i.e. large-scale operation), the ability to regenerate the BC adsorbent in the same column, often more economical and effective, and the ability to achieve a high adsorption rate due to constant contact between the BC adsorbent and fresh fluid [78,79]. Unlike batch adsorption system in which mixing prevalent, for packed bed system mass transport from the bulk fluid to the external surface of the BC adsorbent is generally slow. A packed-bed adsorption column's performance is determined by its breakthrough curve, which is the effluent concentration profile versus time (for a constant flow rate). The breakthrough curve can be obtained either by direct experimentation or by mathematical modelling for any given adsorption system. Generally, adsorbate concentrations leaving the packed-bed column are deemed to have reached the breakthrough point when the concentration reaches 5% of the initial concentration [79]. Mathematical models such as empty bed contact time (EBCT), Bed Depth Service Time (BDST), Adams–Bohart (AB), Thomas (Th), Dose–Response (DR), and Yoon–Nelson (YN) can be applied to study the breakthrough curve behaviour of a packed-bed adsorption column. Due to the simplifications involved in these models and their semi-empirical or empirical nature, the models do not provide full information regarding the design parameters. Therefore, mass transfer models derived from fundamental principles would allow for the simulation of breakthrough curves. Under varied experimental conditions such as influent concentration, inlet flow rate, pH, and bed height, the mass transport (MT) model was evaluated and compared to mathematical models, such as BDST, AB, Th, DR, and YN, to simulate the breakthrough curves of Hg (II) adsorption in a packed-bed adsorption column with ostrich BC [40]. The results showed that the MT model produced the highest accuracy (R^2 = 99.31%, mean residual error (MRE) = 0.745% and normalised root means square error (NRMSE) = 6.15%), and the mathematical models performance can be summarised in the following order: Th > BDST > YN > DR > AB. It was found that maximum adsorption capacity was more sensitive to simulated breakthrough

curves than apparent equilibrium constant and axial dispersion coefficient.

Pilot- and bench-scale fixed-bed adsorption systems were used to compare BC with commercial activated alumina for treating groundwater with 8.5 mg/L naturally occurring fluoride concentration [22]. The results showed that both BC and activated alumina removed fluoride to below 0.1 mg/L. But at the pilot scale for BC and activated alumina, it was found that the fluoride breakthrough was reached within 450 bed volumes (3.1 days) and 650 bed volumes (4.5 days), respectively, when an empty bed contact time (EBCT) of 10 min was employed. This suggests that for industrial scale application using packed beds, BC can perform comparatively as activated alumina if proper strategy for improving its adsorption capacity is applied. On the other hand, it was discovered that fluoride concentrations were higher on BC than activated alumina per square metre of adsorbent surface area, suggesting that maximising BC surface area may enhance adsorption capacity. Methods of improving the surface area of the BC have been reported under the section titled strategies for enhancing adsorption capacity (Section 7). Mesquita et al.[79] reported a fixed-bed adsorption column with BC adsorbent to selectively and partly remove refractory organics, a complex mixture of long-chain hydrocarbons, aromatic compounds, carboxylic acids, amines and amides from electrodialysis concentrate effluent. The result showed that the maximum adsorption capacity increased with the increase in bed depth and reduction in flow rate. The bed depth service time (BDST) model predicted the breakthrough time satisfactorily (deviation near 10%) for C/C_0 of 0.55, 0.60, and 0.65, which can be considered very acceptable. It was also found that the C/C_0 ratios of 0.55, 0.60, and 0.65 could be scaled up to provide a removal efficiency of 45% in 16 days. Recently, Backward Bayesian multiple linear regression (BBMLR) was applied to study the adsorption efficiency of Cd(II) ions by ostrich BC in a packed-bed adsorption column based on the following operational variables consisting of pH, inlet Cd(II) concentration, bed height and feed flow rate [80]. The performance of the BBMLR was evaluated using the coefficient of determination (R^2), NRMSE and MRE. Although the BBMLR model was more sensitive to pH, bed height, and flow rate, it showed excellent performance of NRMSE 6.69% for predicting Cd(II) removal in fixed-bed adsorption systems. BC's adsorption capacity increased as column height increased and decreased as flow rate and initial concentration increased. In another study, the Thomas model (equation 14) and Dose–Response model (equation 15) were used to evaluated the experimental test data, predict the breakthrough curve, and the mechanism of Pb(II) adsorption on BC in a fixed bed column [81]. It was found that the breakthrough curve predicted by the Dose–Response model fit the experimental results well and was significantly better than the predicted results of the Thomas model. At an initial Pb(II) concentration of 200 mg/L, an inlet flow rate of 4 mL/min, and a column height of 30 cm, the maximum adsorption capacity was 38.466 mg/g, and a saturation rate of 95.8% was achieved. As a potential adsorbent, BC can be used to address the problem of water pollution with a packed-bed column on a large scale.

$$\frac{C_t}{C_0} = \frac{1}{1 + exp(\frac{k_{Th} q_0 m}{F} - k_{Th} C_0 t)} \tag{14}$$

where k_{Th} denotes Thomas rate constant (mL/mg min); q_0 the maximum concentration of the solute in the solid phase (i.e. the adsorption capacity of the adsorbent (mg/g)); m the mass of the adsorbent (g); F the flow rate (mL/min); C_0 the initial concentration (mg/L); and t the time. In the Thomas model, reaction kinetics and Langmuir isotherms are hypothesised, but sorption is controlled by interface mass transfer.

$$\frac{C_t}{C_0} = 1 - \frac{1}{1 + (C_0 V / q_0 m)^a} \tag{15}$$

When $b = q_0 m / C_0$, equation 15 becomes equation 16:

$$\frac{C_t}{C_0} = 1 - \frac{1}{1 + (V/b)^a} \tag{16}$$

Where; a and b are the model parameters and V is the solution volume.

Bed Depth Service Time (BDST) model (equation 17) Based on surface chemical reaction theory, the BDST model assumes negligible intraparticle

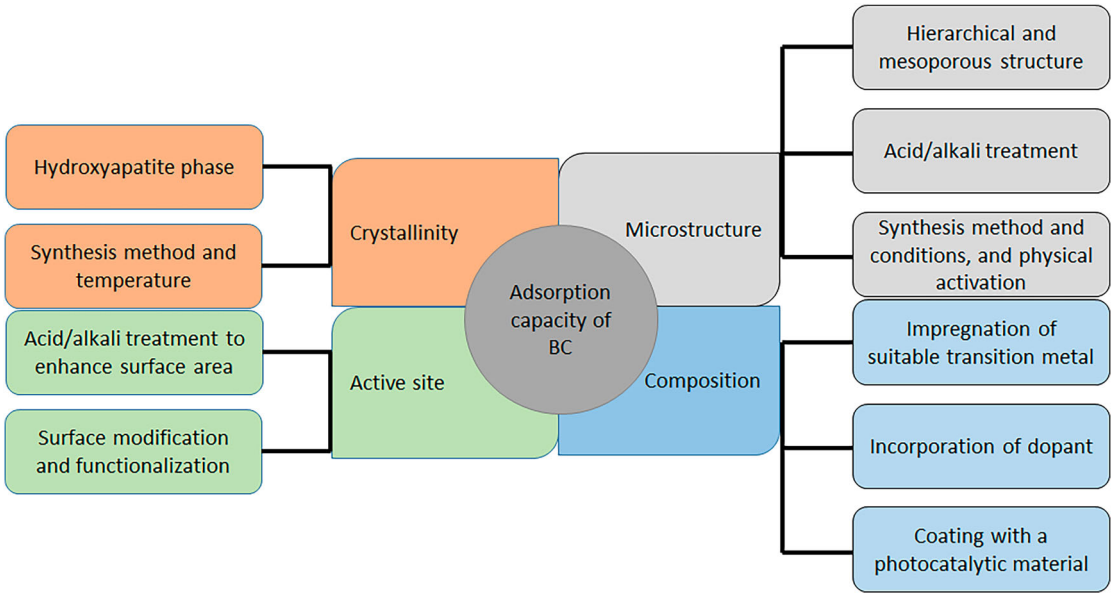

Figure 8. Strategies for enhancing the adsorption capacity of BC.

diffusion and external mass transfer resistance.

$$\frac{C_t}{C_0} = \frac{1}{1 + exp\left[K_{BD}C_0\left(\frac{N_0}{C_0U_0}L - t\right)\right]} \quad (17)$$

where N_0 denotes the maximum adsorption capacity (mg/L), U_0 the linear flow velocity (cm/min), and K_{BD} the adsorption rate constant (L/(mg min)).

7. Strategies for enhancing adsorption capacity of BC

Bone char (BC) can be viewed as a composite of two types of adsorbents (i.e. hydroxyapatite and carbon). It is therefore likely that BC's performance and adsorption capacity will depend on the proportion of total surface provided by each component. There is no doubt that carbon content which is determined by the charring temperature and condition has an impact on BC's performance. Analysis of data from these studies show that BC adsorbents' capacity to remove pollutants is closely related to their physicochemical properties. BC adsorbent morphology and textural attributes such as particle size, pore size distribution, point of zero charge (pH_{PZC}), and specific surface area play a significant role in its performance. Therefore, improving the microstructure, controlling crystallinity, active site (acid/basic sites) and modification of composition will enhance adsorption capacity and performance. Charring temperature affects BC microstructural features, such as pore size distribution and specific surface area. Figure 8 shows the four categories of strategies that can be used to improve the adsorption capacity of BC. Porosity development is expected to be affected by temperature of pyrolysis/gasification of bone constituents. A study of the effects of carbon distribution on hydroxyapatite on BC adsorption is required. It is also possible to increase specific surface area and enhance porous structures by using chemical or physical activation. The physical activation process is carried out at high temperatures (about 600°C) by treating the produced BC in the presence of oxidising gases such as steam, CO_2, and air [43], in order to increase the surface area and pore size distribution. But in chemical activation the bones are treated with acid or alkali prior to or during carbonisation using acid, alkaline or organic solvent. The sorption capacity of bone char can also be enhanced by chemically modifying its surface. Consequently, it is possible to modify a BC's surface properties to achieve specific objectives using surface functionalization. Literature reports have found that hydroxyl and carboxyl groups on the surface of acetic acid-modified BC obtained from cattle and sheep bones effectively adsorb formaldehyde from air polluted with formaldehyde [16]. Based on a study, a BC coated TiO_2 can be applied for photocatalytic activity using salicylic acid as a model water pollutant, giving results that are comparable to suspended TiO_2 nanoparticles

[82]. The results of this study suggest that BC can be used as a green, effective, cheap, and regenerative adsorbent to support photocatalysts for industrial wastewater pollutants degradation. Composition modification can be achieved through impregnation of active metal or incorporation of suitable dopant. BCs for fluoride adsorption from drinking water reportedly synthetised through metallic doping using aluminium and iron salts [83]. It was reported that when aluminium sulfate was used to modify the composition and surface of BC, fluoride adsorption was enhanced by 600% and adsorption capacity of 31 mg/g. There is a possibility that these surface interactions could involve an ion exchange between the fluoride ion (F^-) and the OH^- from Al–OH and Ca–OH bonds during water defluoridation. Furthermore, cerium species have been used to modify the surface chemistry of BC and its application as an adsorbent for fluoride investigated [84]. The result showed that the incorporation of cerium (Ce^{4+}) enhanced fluoride adsorption properties of BC up to 13.6 mg/g.

Adsorption of the Direct Brown 166 dye (DB-166) from aqueous solutions was investigated using a natural chitosan/BC composite [85]. The maximum adsorption efficiency and capacity were found as thus 99.8% and 21.18 mg/g, respectively. The results indicate that impregnation and incorporation of dopants can modify BC's composition and surface chemistry. According to one study, nano-sized manganese modified BC surfaces provide 78 times higher adsorption capacity (maximum adsorption capacity 9.46 mg/g) for As(V) removal compared to uncoated BC, and the effectiveness of the removal increases linearly as manganese concentration increases from 0.025 to 14.5 mg/g [86]. Furthermore, microcrystalline cellulose-modified bone char (MCC-BC) and BC were investigated as adsorbents for the removal of Pb (II) from solution, and it was found that BC had a maximum adsorption capacity of 89.9 mg/g, while MCC-BC had 115.7 mg/g [87]. According to the results, the MCC-BC has a higher adsorption capacity, a shorter adsorption time, and a better adsorption and reusability performance than BC (without surface modification). The mechanisms of removal include chemical precipitation of Ca_x-$Pb_{(10-x)}(PO_4)_6(OH)_2$ by ion exchange of Ca (II) and Pb (II), accompanied by the coordination of Pb (II) with hydroxyl groups on the BC surface, which fitted Langmuir model and single-layer chemical adsorption. Also, composites containing BC from cattle, Fe_3O_4 nanoparticles (<50 nm) and chitosan biopolymer were reported to be effective in adsorbing As (V) in aqueous solutions at pH 2–11 [88]. According to this study, the mechanism of adsorption involves electrostatic interaction between negatively charged As(V) species and positively charged $Fe_3O_4^-$ nanocomposite BC surface. On the other hand, BC produced by paralysing from 350°C to 700°C demonstrated a lower temperature causes a higher fluoride adsorption capacity [89]. The dehydroxylation of the hydroxyapatite in BC is thought to be the main reason for the inverse correlation between fluoride adsorption and pyrolysis temperature. However, bones with charring temperatures below 300°C retain some organic matter, and also the specific surface area and pore structure of the produced BC is not well developed, as shown in Figure 1 [90]. The physicochemical properties and mesoporous structure of BC can be improved through chemical activation using either H_3PO_4, H_2SO_4, KOH, NaOH or K_2CO_3 and gasification reactions [15,91,92]. Research has shown that acid or alkali treatment can increase porosity by about 30% and the surface area up to 234 m^2/g (i.e. 20%–30% increase) compared to non-alkali-treated in BC derived material [91]. This confirms that acid or alkali treatment of BC adsorbent enhances pore structure network and surface area. The same literature also reported that treatment with KOH lowers the PZC of BC from 7.7 to −5.6, which favours the generation of acid functional groups on surface. By treating BC with H_2SO_4, a highly microporous material was obtained, suitable for adsorption of gaseous pollutants, but NaOH and K_2CO_3, on the other hand, resulted in a hierarchical porous structure, with a greater equilibration increase in microporosity and mesoporosity [92]. Under the operating conditions used, it was observed that H_3PO_4 was extremely aggressive, removing almost all the BC's pores. In another study, it was discovered that acid treatment at 0.2 mmol(H_2SO_4)/g(BC) increased surface area by about 80% due to enhanced microporosity by up to 263% compared to untreated BC [15]. These results prove that with appropriate optimisation of synthesis method and a suitable treatment solvent, the porous structure and textural properties of the BC can be configured from microporosity to macroporosity

depending on the molecular size of the pollutants and adsorption application.

8. Regeneration of bone char (BC)

For evaluating the application and lifespan of BC, regeneration methods are necessary, which reduce the cost of the process and reduce the amount of unwanted waste. The regeneration of an adsorbent plays an important role in its evaluation. This aspect has only been reported in a few studies, which may limit industrial applications of BC. Studies have been conducted on the thermal and chemical regeneration of fluoride saturated BC [93,94]. As both methods can be performed in situ, unloading, transporting, and reconditioning of the adsorbent are eliminated. A sustainable adsorbent material is demonstrated by regeneration. It is critical to measure BC's regeneration capacity in order to assess its reusability and effectiveness in removing contaminants from water or gas purification.

The thermal method involves heating the pollutant saturated BC under a purge gas flow, which removes the desorbed adsorbate and facilitate regeneration for multiple cycles. Saturated BC can also be regenerated thermally using boiling water or steam [93]. As a result of regeneration, pollutants that are adhered to the surface of the BC move into its exterior, exposing more active surfaces for adsorption. In this thermal regeneration process, no chemical agents are used and no waste products are produced, so there are almost no emissions. The effect of regeneration temperature, regeneration duration, and regenerated BC adsorption capacity has been investigated and published in the literature for the thermal method [94]. It was found that the regenerated BC with a temperature of 500°C for 2 h had the best fluoride sorption potential. The results of another study showed that 400°C was the optimal temperature for thermal regeneration for fluorine saturated BC [95,96]. It has been found that fluoride ions were diffused into BC particles during thermal regeneration [95]. As a result, fluorated hydroxyapatite is formed, indicating that fluoride has been incorporated into hydroxyapatite structures in BC due to thermal treatment. In another study, BC's structure remained unchanged even after five continuous regeneration cycles at 400°C, based on X-ray diffraction (XRD) patterns before and after [96]. This suggests that the incorporation of fluorine into BC depends on the regeneration temperature applied. Also, the loss of some carbon component of the BC resulting from thermal regeneration is possible. However, analysis showed an increase in the degree of crystallinity of BC following thermal regeneration. After thermal regeneration, BC showed a slight decrease in adsorption capacity. Adsorption equilibrium cannot be completely reversed, as desorption depends on the mechanism by which the pollutant is adsorbed, whether physisorption or chemisorption on BC surface.

In contrast, regeneration of pollutant saturated BC can be carried out with the aid of suitable chemical solvents such as sodium hydroxide (NaOH) for fluorine saturated BC. Organic solvents and inorganic chemicals can both be used as chemical regenerating agents. Nigri et al. [97] reported the regeneration of fluorine saturated BC using NaOH (0.5 mol/L) solution. Observation of a 30% reduction in adsorption capacity after five cycles of adsorption/desorption was observed. A plot of the regeneration efficiency against concentration of NaOH showed that for 0.2 mol·dm^{-3} NaOH, an efficiency of 91.2% could be achieved [45]. It is found that removing adsorbed F^- ions from the BC surface is more efficient when a solution of NaOH is used at a high concentration. In other words, the mechanism of desorption involves ion-exchange of OH^- group (NaOH) with fluoride ions on BC adsorbent. Among the factors influencing fluoride removal, pH played the biggest role. Hence, chemical solvent regeneration process is pH dependent. In fluoride removal, for instance, fluoride ions exchange with hydroxyl, carbonate, hydrogen carbonate, and phosphate ions of BC. Research has been conducted on the effectiveness of different sodium solutions (NaOH, Na_2CO_3, $NaHCO_3$ and Na_3PO_4) in rejuvenating fluoride-saturated BC for reuse in fluoride removal from drinking water [98]. The effect of temperature on rejuvenation process was also studied. It was found that NaOH exhibited the highest de-fluoridation effectiveness while the lowest was $NaHCO_3$. Results show that BC releases more fluoride when the temperature is raised from 20°C to 60°C during regeneration. In 2020, Coltre et al. [99] reported the application of aqueous solutions with pH from 2 to 12 and alcoholic solutions of methyl, ethyl and isopropyl as regenerating agents in a batch system with a constant temperature

of 30°C for BC saturated with blue BF-5G dye. As a result of improved regeneration efficiency, isopropyl and ethyl alcohols achieved about 21.0% and 19.5%, respectively. It is therefore reasonable to conclude that the interactions between the pollutant and the BC surface play a significant role in the selection of chemical solvents. With this regeneration method, the recovery of the adsorbate from the BC is possible. It is, however, a complicated process that can result in the release of harmful chemicals into the environment following chemical reactions. Consequently, the efficiency of regeneration is very low.

9. Future outlook

The demand for high-performance, sustainable, and renewable adsorbents, heterogeneous catalysts, and hierarchical porous carbon microstructures is increasing. To address today's environmental problems, such as clean water, clean energy and emission control, green and sustainable adsorbents and catalysts are critical. BC is more suitable for use as a catalyst support when its physicochemical properties are improved. The adsorption capacity of BC depends more on its surface area than on its hydroxyapatite content. To achieve this, a chemical modification of BC with an acid or alkali can potentially increase the surface area and pore distribution and increase its adsorption capacity. There is still a need to investigate the impact of different chemical treatments (i.e., alkali and acid treatments) on the textural properties of BC, including porosity, pore size distribution, and surface area. It would be interesting to investigate how to combine strong adsorptive BC with photocatalyst material to degrade organic pollutants. The study should include preparation, characterisation and investigation as a carrier for photocatalysts in a photocatalytic composite. This viewpoint suggests combining BC with photocatalytic materials such as ZnO and TiO_2 or a composite with other suitable photocatalytic precursor in the form ZnO/BC [100,101]. A suitable photocatalytic material precursor will be precipitated on BC as part of the synthesis process for composite photocatalyst. Photocatalytic oxidation is used in green degradation technology to remove heavy metals and oxidise organic compounds. A synergistic effect has been demonstrated between the immobilisation of ZnO nanoparticles on BC and the photocatalytic degradation of formaldehyde, an air pollutant [102]. As a result of the strong adsorption of pollutant molecules on BC surfaces, there would be a higher transport rate to the photocatalytic material. This would lead to a higher rate of photocatalysis as well as pollutant degradation. As a result, future outlook will include modifying bone-derived adsorbents into photocatalysts and applying them to degrade organic pollutants from industrial wastewater.

A quality BC should exhibit the following characteristics: (1) a high capacity for absorbing pollutants, (2) low organic matter content, and (3) no fecal contamination in storage or production. Investigation of the technicalities surrounding the collection of waste bones is essential to reducing the environmental impact and boosting economic benefits. Furthermore, the acidity or basicity of the BC surface plays a major role in the adsorption of molecules. BC's acidic-basic properties play a crucial role during adsorption, since it determines how molecules interact and adsorb onto the surface. It is necessary to examine the impact of the acid–base property of BC in order to gain a mechanistic understanding of the role surface chemistry on adsorption. Research is also needed to determine the impact of process type and conditions on acidity-basicity, as well as adsorption capacity, of BC produced. A study of the nature of thermodynamic parameters involved in pollutant adsorption onto BC. Additionally, further research is needed on how valorising methods, the effect of bone type (i.e. soft and hard) and source, and process conditions affect BC's physicochemical and textural properties in relation to its adsorption capacity. It is critical to note that the BC adsorbent's physicochemical properties are highly impacted by the conditions under which it is synthesised, and can vary significantly from pollutant to pollutant. In both an economic and technical point of view, it makes sense to tailor the physicochemical properties of BC adsorbents for water treatment and air purification. Variations in the synthesis routes and conditions lead to high variability in the physicochemical properties of the final BC. Further study of the effects of production conditions in the preparation of BC and the parameters that affect its adsorption properties to different pollutants from aqueous solutions and the air is required. BC adsorbent performance and production costs can be improved by optimising synthesis conditions and tailor adsorption properties based on pollutant. Likewise, further research is

needed to determine how BC's functionalization affects adsorption capacity and catalytic performance. As far as environmental impacts of bone char production are concerned, no studies have been conducted. The current production process must be evaluated along with a cost–benefit analysis in order to determine if it is environmentally friendly or not. As well, life-cycle assessment and techno-economic modelling can be utilised to evaluate the cost implications of valorising waste bones on a large scale.

10. Conclusion

Waste bone biomass is one of the largest waste products in livestock production, and it can be recycled and utilised as hydroxyapatite material or bone char (BC) to ensure sustainable environment and solid waste management. Contaminants can be removed from water, gaseous effluents and soil through adsorption using BC produced *via* thermochemical processes such as calcination, pyrolysis, or gasification of waste bones. As a result of its low-cost and high efficiency, BC adsorption technology can be applied widely for the treatment of wastewater and contaminated soil remediation. BC has demonstrated mesoporosity and surface chemistry due to the presence of several functional groups, which enhances its adsorption capabilities in removing numerous contaminants from wastewater. BC adsorbs pollutants mainly through its hydroxyapatite component, and hydroxyapatite adsorption sites are formed by the subsequent protonation and deprotonation reaction depending on pH_{PZC} and solution pH. This study critically analyses the results of relevant researches, and assembles and evaluates data related to the use of BC adsorbents based on both empirical and theoretical methodologies. By providing theoretical adsorption mechanisms, strategies for increasing BC adsorption capacity, and future outlook, this study serves as a guide for further research and development of environmentally friendly, and low-cost adsorbent to tackle water pollution and gas purification/air pollution problems.

Based on equilibrium sorption isotherms, the BC adsorption system's capacity and performance can be predicted. In nonlinear regression, the difference between experimental measurements and the mathematical model is minimised (or maximised). It is generally preferred to select the best-fitting isotherm model based on which error function produces the lowest error distribution between the model predicted and measured experimental values. It has been demonstrated that nonlinear regression is the best method for obtaining the parameters of isotherm equations and choosing the optimum model. In order to evaluate the accuracy of error functions in predicting the isotherm parameter values, as well as the optimum isotherm, an extensive and detailed study has to be conducted for BC adsorbent.

No studies have been conducted to determine the environmental impacts of bone char production. An assessment of these impacts along with a cost–benefit analysis is necessary to determine whether the current production process is economical or harmful to the environment. Future research should therefore focus on life cycle assessment (LCA), which is a quantitative method that can be used to evaluate the environmental impact and economic analysis of BC production over its lifetime. The application of machine learning and artificial neural networks to modelling adsorption data and isotherms is another area to be investigated. Currently, BC adsorption studies are generally concentrated on batch or equilibrium studies, which may be difficult to cover to commercial-scale applications, so future studies should emphasise pilot- and fixed-bed adsorption experiments. Simulations and computational analyses of adsorption and diffusion on BC adsorbents for various adsorbates is an interesting topic requiring further exploration. There is a need to investigate further the components of BC carbon and/or hydroxyapatite responsible for the adsorption of a pollutant. Another area which needs further research is how functionalization of BC affects adsorption capacity and catalytic activity.

Author contributions

Conceptualisation and design: AH, writing–original draft: AH and DWP; writing review and editing: AH, DWP, SO, and EP; data collection and analysis: DWP, SO, AH and EP; supervision: AH. All authors read and approved the final manuscript.

Disclosure statement

No potential conflict of interest was reported by the author(s).

Consent to participate

The authors of this paper have given their consent to participate in its writing and submission.

Consent to publish

This paper has been approved by all authors and their consent has been given for its publication.

Notes on contributors

Dr Abarasi Hart qualified with a BEng in Chemical Engineering from Niger Delta University in 2006. His MSc in Advanced Chemical Engineering was earned in 2010, and his PhD in Advanced Studies of Catalytic Upgrading of Heavy Oils was awarded in 2014, both from the University of Birmingham, UK. Dr Hart worked as a lecturer at the Department of Chemical Engineering, University of Port Harcourt (2008–2012). A research fellow at the University of Birmingham from 2014 to 2020, research associate at the Department of Chemical and Biological Engineering, the University of Sheffield (2021–2023), and currently, he is a research associate at the Department of Chemical Engineering and Applied Chemistry, Aston University, UK. His research focuses on applied catalysis, heavy oil recovery and upgrading, catalytic upgrading of bio-oil into hydrocarbon fuels and sustainable chemicals, waste-to-materials, waste-to-energy, biomass conversion, energy materials, and food processing.

Dr Duduna William Porbeni is a lecturer in the Department of Chemical Engineering, Faculty of Engineering, Niger Delta University, Bayelsa, Nigeria. She qualifies with BEng (Niger Delta University, Nigeria), MSc (University of Surrey, UK) and PhD (Niger Delta University, Nigeria). Her research interest lies on environmental pollution control and waste management, water and wastewater research, and microbial concrete corrosion engineering.

Dr Selina Omonmhenle is an Associate Professor in the Department of Chemistry, Faculty of Physical Sciences, University of Benin, Benin city. She qualified with B.Ed, Sc. (Chemistry) from University of Benin, Nigeria in 1990. She completed her master's degree in Industrial Chemistry from the University of Benin, Nigeria in 1995. She obtained a PhD in Chemistry from the University of Birmingham, UK in 2014. Her research interest focuses on the design and development of hybrid materials and nanomaterials with improved functionalities comprising a wide range of cationic and anionic clays, natural and synthetic clays as multifunctional materials with varied applications: adsorbents, catalysts, nanocomposites, drug delivery system, agrochemicals etc. Biomas conversion and waste to materials for variety of applications with emphasis on industries and environment.

Mr Ebikapaye Peretomode is a PhD candidate at Robert Gordon University, Aberdeen, UK. He holds an MSc in Petroleum Engineering from the London South Bank University, UK. He obtained a BEng in Chemical Engineering from the Niger Delta University, Bayelsa state, Nigeria. His research interest includes biomaterials, fluid–rock interaction and reservoir geomechanics.

References

[1] Hart A, Ebiundu K, Peretomode E, et al. Value-added materials recovered from waste bone biomass: technologies and applications. RSC Adv. 2022;12(34):22302–22330. doi:10.1039/d2ra03557j.

[2] A. Hart and E. Aliu, Materials from eggshells and animal bones and their catalytic applications. In: Minh Doan Pham, editor. Design and applications of hydroxyapatite-based catalysts. Boschstr. 12, 69469 Weinheim, Germany: John Wiley & Sons; 2022. p. 437–479.

[3] A. Hart and H. Onyeaka, Carbon capture. In: Khan SAR, editor. Eggshell and seashells biomaterials sorbent for carbon dioxide capture. London: IntechOpen; 2020. p. 83–94.

[4] Rojas-Mayorga CK, et al. Optimization of pyrolysis conditions and adsorption properties of bone char for fluoride removal from water. J Anal Appl Pyrolysis. 2013;104:10–18. doi:10.1016/j.jaap.2013.09.018.

[5] Hart A. Mini-review of waste shell-derived materials' applications. Waste Manag Res. 2020;38(5):514–527. doi:10.1177/0734242X19897812.

[6] Hart A. Circular economy : closing the catalyst loop with metal reclamation from spent catalysts, industrial waste, waste shells and animal bones. Biomass Convers Biorefinery. 2021. doi:10.1007/s13399-021-01942-8.

[7] Azeem M, et al. Removal of potentially toxic elements from contaminated soil and water using bone char compared to plant- and bone-derived biochars: A review. J Hazard Mater. 2022;427:128131, doi:10.1016/j.jhazmat.2021.128131.

[8] Bennett MC, Abram JC. Adsorption from solution on the carbon and hydroxyapatite components of bone char. J Colloid Interface Sci. 1967;23(4):513–521. doi:10.1016/0021-9797(67)90198-1.

[9] Hyder AHMG, Begum SA, Egiebor NO. Adsorption isotherm and kinetic studies of hexavalent chromium removal from aqueous solution onto bone char. J Environ Chem Eng. 2015;3(2):1329–1336. doi:10.1016/j.jece.2014.12.005.

[10] Rojas-Mayorga CK, Mendoza-Castillo DI, Bonilla-Petriciolet A, et al. Tailoring the adsorption behavior of bone char for heavy metal removal from aqueous solution. Adsorpt Sci Technol. 2016;34(6):368–387. doi:10.1177/0263617416658891.

[11] Yami TL, Du J, Brunson LR, et al. Life cycle assessment of adsorbents for fluoride removal from drinking water in East Africa. Int J Life Cycle Assess. 2015;20(9):1277–1286. doi:10.1007/s11367-015-0920-9.

[12] Someus E, Pugliese M. Concentrated phosphorus recovery from food grade animal bones. Sustain. 2018;10 (7):1–17. doi:10.3390/su10072349.
[13] Medellin-Castillo NA, et al. Adsorption of fluoride from water solution on bone char. Ind Eng Chem Res. 2007;46(26):9205–9212. doi:10.1021/ie070023n.
[14] Alkurdi SSA, Al-Juboori RA, Bundschuh J, et al. Bone char as a green sorbent for removing health threatening fluoride from drinking water. Environ Int. 2019;127:704–719. doi:10.1016/j.envint.2019.03.065.
[15] Iriarte-Velasco U, Sierra I, Zudaire L, et al. Preparation of a porous biochar from the acid activation of pork bones. Food Bioprod Process. 2016;98:341–353. doi:10.1016/j.fbp.2016.03.003.
[16] Rezaee A, Rangkooy H, Jonidi-Jafari A, et al. Surface modification of bone char for removal of formaldehyde from air. Appl Surf Sci. 2013;286:235–239. doi:10.1016/j.apsusc.2013.09.053.
[17] Wang M, Liu Y, Yao Y, et al. Comparative evaluation of bone chars derived from bovine parts: physicochemical properties and copper sorption behavior. Sci Total Environ. 2020;700:134470, doi:10.1016/j.scitotenv.2019.134470.
[18] Wang J, Guo X. Adsorption isotherm models: classification, physical meaning, application and solving method. Chemosphere. 2020;258:127279, doi:10.1016/j.chemosphere.2020.127279.
[19] Abe I, Iwasaki S, Tokimoto T, et al. Adsorption of fluoride ions onto carbonaceous materials. J Colloid Interface Sci. 2004;275:35–39. doi:10.1016/j.jcis.2003.12.031.
[20] Rezaee A, Ghanizadeh G, Behzadiyannejad G, et al. Adsorption of endotoxin from aqueous solution using bone char. Bull Environ Contam Toxicol. 2009;82 (6):732–737. doi:10.1007/s00128-009-9690-z.
[21] Medellin-Castillo NA, et al. Removal of fluoride from aqueous solution using acid and thermally treated bone char. Adsorption. 2016;22:951–961. doi:10.1007/s10450-016-9802-0.
[22] Kennedy AM, Arias-Paic M. Fixed-bed adsorption comparisons of bone char and activated alumina for the removal of fluoride from drinking water. J Environ Eng. 2020;146(1):04019099, doi:10.1061/(asce)ee.1943-7870.0001625.
[23] Chen YN, Chai LY, De Shu Y. Study of arsenic(V) adsorption on bone char from aqueous solution. J Hazard Mater. 2008;160(1):168–172. doi:10.1016/j.jhazmat.2008.02.120.
[24] Liu J, Huang X, Liu J, et al. Adsorption of arsenic(V) on bone char: batch, column and modeling studies. Environ Earth Sci. 2014;72(6):2081–2090. doi:10.1007/s12665-014-3116-x.
[25] Alkurdi SSA, Al-juboori RA, Bundschuh J, et al. Inorganic arsenic species removal from water using bone char : a detailed study on adsorption kinetic and isotherm models using error functions analysis. J Hazard Mater. 2021;405(July 2020):124112, doi:10.1016/j.jhazmat.2020.124112.
[26] Moreno JC, Gómez R, Giraldo L. Removal of Mn, Fe, Ni and Cu ions from wastewater using cow bone charcoal. Materials (Basel). 2010;3(1):452–466. doi:10.3390/ma3010452.
[27] Hassan SSM, Awwad NS, Aboterika AHA. Removal of mercury(II) from wastewater using camel bone charcoal. J Hazard Mater. 2008;154(1–3):992–997. doi:10.1016/j.jhazmat.2007.11.003.
[28] Slimani R, El Ouahabi I, Elmchaouri A, et al. Adsorption of copper (II) and zinc (II) onto calcined animal bone meal. Part I: kinetic and thermodynamic parameters. Chem Data Collect. 2017;9–10:184–196. doi:10.1016/j.cdc.2017.06.006.
[29] Ghaneian MT, Ghanizadeh G, Alizadeh MTH, et al. Equilibrium and kinetics of phosphorous adsorption onto bone charcoal from aqueous solution. Environ Technol. 2014;35(7):882–890. doi:10.1080/09593330.2013.854838.
[30] Kasim NZ, Abd Malek NAA, Hairul Anuwar NS, et al. Adsorptive removal of phosphate from aqueous solution using waste chicken bone and waste cockle shell. Mater Today Proc. 2020;31:A1–A5. doi:10.1016/j.matpr.2020.09.687.
[31] Yang Y, Sun C, Lin B, et al. Surface modified and activated waste bone char for rapid and efficient VOCs adsorption. Chemosphere. 2020;256:127054, doi:10.1016/j.chemosphere.2020.127054.
[32] Becerra-Pérez O, et al. Energy-saving and sustainable separation of bioalcohols by adsorption on bone char. Adsorpt Sci Technol. 2021;2021(Article ID 6615766):16, doi:10.1155/2021/6615766.
[33] Jia P, Tan H, Liu K, et al. Removal of methylene blue from aqueous solution by bone char. Appl Sci. 2018;8 (10):1903, doi:10.3390/app8101903.
[34] Jia P, Tan H, Liu K, et al. Enhanced photocatalytic performance of ZnO/bone char composites. Mater Lett. 2017;205:233–235. doi:10.1016/j.matlet.2017.06.099.
[35] Zhou X, et al. Persulfate activation by swine bone char-derived hierarchical porous carbon: multiple mechanism system for organic pollutant degradation in aqueous media. Chem Eng J. 2020;383:123091, doi:10.1016/j.cej.2019.123091.
[36] Reynel-Avila HE, Mendoza-Castillo DI, Bonilla-Petriciolet A. Relevance of anionic dye properties on water decolorization performance using bone char: adsorption kinetics, isotherms and breakthrough curves. J Mol Liq. 2016;219:425–434. doi:10.1016/j.molliq.2016.03.051.
[37] Ayawei N, Ebelegi AN, Wankasi D. Modelling and interpretation of adsorption isotherms. J Chem. 2017;2017(Article ID 3039817):11, doi:10.1155/2017/3039817.
[38] Foo KY, Hameed BH. Insights into the modeling of adsorption isotherm systems. Chem Eng J. 2010;156:2–10. doi:10.1016/j.cej.2009.09.013.

[39] Ko DCK, Cheung CW, Choy KKH, et al. Sorption equilibria of metal ions on bone char. Chemosphere. 2004;54 (3):273–281. doi:10.1016/j.chemosphere.2003.08.004.

[40] Amiri MJ, Bahrami M, Nekouee N. Analysis of breakthrough curve performance using theoretical and empirical models: Hg2+ removal by bone char from synthetic and real water. Arab J Sci Eng. 2022. doi:10.1007/s13369-022-07432-x.

[41] Amiri MJ, Bahrami M, Dehkhodaie F. Optimization of Hg(II) adsorption on bio-apatite based materials using CCD-RSM design: characterization and mechanism studies. J Water Health. 2019;17(4):556–567. doi:10.2166/wh.2019.039.

[42] Cruz-Briano SA, Medellín-Castillo NA, Torres?Dosal A, et al. Bone char from an invasive aquatic specie as a green adsorbent for fluoride removal in drinking water. Water Air Soil Pollut. 2021;232(9):346, doi:10.1007/s11270-021-05286-x.

[43] Zhu L, Shen D, Luo KH. A critical review on VOCs adsorption by different porous materials: species, mechanisms and modification methods. J Hazard Mater. 2020;389(5 May 2020):122102, doi:10.1016/j.jhazmat.2020.122102.

[44] Saffari M, Moazallahi M. Evaluation of slow-pyrolysis process effect on adsorption characteristics of cow bone for Ni ion removal from Ni- contaminated aqueous solutions. Pollution. 2022;8(3):1076–1087. doi:10.22059/POLL.2022.339417.1377.

[45] Hu J, Wu D, Rao R, et al. Adsorption kinetics of fluoride on bone char and its regeneration. Environ Prot Eng. 2017;43(3):93–112. doi:10.5277/epe170306.

[46] Yang W, Luo W, Sun T, et al. Adsorption performance of Cd(II) by chitosan-Fe3O4-modified fish bone char. Int J Environ Res Public Health. 2022;19:1260.

[47] Patel S, Han J, Qiu W, et al. Journal of Environmental Chemical Engineering Synthesis and characterisation of mesoporous bone char obtained by pyrolysis of animal bones, for environmental application. Biochem Pharmacol. 2015;3(4):2368–2377. doi:10.1016/j.jece.2015.07.031.

[48] Dela Piccolla C, Hesterberg D, Muraoka T, et al. Optimizing pyrolysis conditions for recycling pig bones into phosphate fertilizer. Waste Manag. 2021;131 (November 2020):249–257. doi:10.1016/j.wasman.2021.06.012.

[49] Alkurdi S, Al-Juboori R, Bundschuh J, et al. Evaluating the ability of bone char/nTiO2 composite and UV radiation for simultaneous oxidation and adsorption of arsenite. Sustain Chem. 2022;3(1):19–34. doi:10.3390/suschem3010002.

[50] Malla KP, et al. Extraction and characterization of novel natural hydroxyapatite bioceramic by thermal decomposition of waste ostrich bone. Int J Biomater. 2020;2020:1690178, doi:10.1155/2020/1690178.

[51] Abifarin JK, Obada DO, Dauda ET, et al. Experimental data on the characterization of hydroxyapatite synthesized from biowastes. Data Br. 2019;26:104485, doi:10.1016/j.dib.2019.104485.

[52] Guo Q, Tang H, Jiang L, et al. Sorption of Cd2 + on bone chars with or without hydrogen peroxide treatment under various pyrolysis temperatures: comparison of mechanisms and performance. Processes. 2022;10 (4):618, doi:10.3390/pr10040618.

[53] Hernández-Barreto DF, Hernández-Cocoletzi H, Moreno-Piraján JC. Biogenic hydroxyapatite obtained from bone wastes using CO2 – assisted pyrolysis and its interaction with glyphosate : a computational and experimental study. ACS Omega. 2022;7:23265–23275. doi:10.1021/acsomega.2c01379.

[54] Choy KKH, Ko DCK, Cheung CW, et al. Film and intraparticle mass transfer during the adsorption of metal ions onto bone char. J Colloid Interface Sci. 2004;271:284–295. doi:10.1016/j.jcis.2003.12.015.

[55] Inglezakis VJ, Balsamo M, Montagnaro F. Liquid – solid mass transfer in adsorption systems—an overlooked resistance ? Ind Eng Chem Res. 2020;59(50):22007–22016. doi:10.1021/acs.iecr.0c05032.

[56] Gai WZ, Deng ZY. A comprehensive review of adsorbents for fluoride removal from water: performance, water quality assessment and mechanism. Environ Sci Water Res Technol. 2021;7(8):1362–1386. doi:10.1039/d1ew00232e.

[57] Nasrollahzadeh M, Soheili Bidgoli NS, Shafiei N, et al. Low-cost and sustainable (nano)catalysts derived from bone waste: catalytic applications and biofuels production. Biofuels, Bioprod Biorefining. 2020;14(6):1197–1227. doi:10.1002/bbb.2138.

[58] Chojnacka K. Equilibrium and kinetic modelling of chromium(III) sorption by animal bones. Chemosphere. 2005;59(3):315–320. doi:10.1016/j.chemosphere.2004.10.052.

[59] Deydier E, Guilet R, Sharrock P. Beneficial use of meat and bone meal combustion residue: 'an efficient low cost material to remove lead from aqueous effluent'. J Hazard Mater. 2003;101(1):55–64. doi:10.1016/S0304-3894(03)00137-7.

[60] Elvir-padilla LG, Mendoza-castillo DI. Adsorption of dental clinic pollutants using bone char : adsorbent preparation, assessment and mechanism analysis. Chem Eng Res Des. 2022;183:192–202. doi: 10.1016/j.cherd.2022.05.003.

[61] Villela-Martínez DE, Leyva-Ramos R, Aragón-Piña A, et al. Arsenic elimination from water solutions by adsorption on bone char. Effect of operating conditions and removal from actual drinking water. Water Air Soil Pollut. 2020;231(5):201, doi:10.1007/s11270-020-04596-w.

[62] Alkurdi SSA, Herath I, Bundschuh J, et al. Biochar versus bone char for a sustainable inorganic arsenic mitigation in water: what needs to be done in future research? Environ Int. 2019;127(June 2019):52–69. doi:10.1016/j.envint.2019.03.012.

[63] Al-Sou'od K. Kinetics of the adsorption of hexavalent chromium from aqueous solutions on low cost material.

African J Pure Appl Chem. 2012;6:190–197. doi:10.5897/AJPAC12.064.

[64] Wang J, Guo X. Adsorption kinetic models : physical meanings, applications, and solving methods. J Hazard Mater. 2020;390(November 2019):122156, doi:10.1016/j.jhazmat.2020.122156.

[65] Chu KH. Revisiting the Temkin isotherm : dimensional inconsistency and approximate forms. Ind Eng Chem Res. 2021;60(35):13140–13147. doi:10.1021/acs.iecr.1c01788.

[66] Cheung CW, Porter JF, Mckay G. Sorption kinetic analysis for the removal of cadmium ions from effluents using bone char. Water Res. 2001;35(3):605–612. doi:10.1016/S0043-1354(00)00306-7.

[67] Nigri EM, Cechinel PAM, Mayer AD, et al. Cow bones char as a green sorbent for fluorides removal from aqueous solutions : batch and fixed-bed studies. Environ Sci Pollut Res. 2017;24:2364–2380. doi:10.1007/s11356-016-7816-5.

[68] Bedin KC, de Azevedo SP, Leandro PKT, et al. Bone char prepared by CO2 atmosphere: preparation optimization and adsorption studies of Remazol Brilliant Blue R. J Clean Prod. 2017;161:288–298. doi:10.1016/j.jclepro.2017.05.093.

[69] Pan X, Wang J, Zhang D. Sorption of cobalt to bone char: kinetics, competitive sorption and mechanism. Desalination. 2009;249(2):609–614. doi:10.1016/j.desal.2009.01.027.

[70] de Melo NH, de Oliveira Ferreira ME, Silva Neto EM, et al. Evaluation of the adsorption process using activated bone char functionalized with magnetite nanoparticles. Environ Nanotechnol Monit Manag. 2018;10 (December 2018):427–434. doi:10.1016/j.enmm.2018.10.005.

[71] Patel S, Han J, Gao W. Sorption of 17β-estradiol from aqueous solutions on to bone char derived from waste cattle bones: kinetics and isotherms. J Environ Chem Eng. 2015;3(3):1562–1569. doi:10.1016/j.jece.2015.04.027.

[72] Cheung CW, Porter JF, McKay G. Removal of Cu(II) and Zn(II) ions by sorption onto bone char using batch agitation. Langmuir. 2002;18(3):650–656.

[73] Li Y, Wang M, Liu J, et al. Adsorption/desorption behavior of ionic dyes on sintered bone char. Mater Chem Phys. 2023;297(January):127405. doi:10.1016/j.matchemphys.2023.127405.

[74] Moussavi SP, et al. Superior removal of humic acid from aqueous stream using novel calf bones charcoal nanoadsorbent in a reversible process. Chemosphere. 2022;301(March):134673. doi:10.1016/j.chemosphere.2022.134673.

[75] Subramanyam B, Das A. Linearised and non-linearised isotherm models optimization analysis by error functions and statistical means. J Environ Heal Sci Eng. 2014;12:19.

[76] Sreńscek-Nazzal J, Narkiewicz U, Morawski AW, et al. Comparison of optimized isotherm models and error functions for carbon dioxide adsorption on activated carbon. J Chem Eng Data. 2015;60(11):3148–3158. doi:10.1021/acs.jced.5b00294.

[77] Kumar KV, Porkodi K, Rocha F. Comparison of various error functions in predicting the optimum isotherm by linear and non-linear regression analysis for the sorption of basic red 9 by activated carbon. J Hazard Mater. 2008;150(1):158–165. doi:10.1016/j.jhazmat.2007.09.020.

[78] Tovar-Gómez R, Moreno-Virgen MR, Dena-Aguilar JA, et al. Modeling of fixed-bed adsorption of fluoride on bone char using a hybrid neural network approach. Chem Eng J. 2013;228:1098–1109. doi:10.1016/j.cej.2013.05.080.

[79] Mesquita PDL, Souza CR, Santos NTG, et al. Fixed-bed study for bone char adsorptive removal of refractory organics from electrodialysis concentrate produced by petroleum refinery. Environ Technol (United Kingdom). 2018;39(12):1544–1556. doi:10.1080/09593330.2017.1332691.

[80] Amiri MJ, Mahmoudi MR, Khozaei M. Fixed bed column modeling of Cd(II) adsorption on bone char using backward Bayesian multiple linear regression. Pollution. 2020;6(2):441–451. doi:10.22059/POLL.2020.294364.727.

[81] Li G, Zhang J, Liu J, et al. Investigation of the transport characteristics of Pb(II) in sand-bone char columns. Sci Prog. 2021;104(2):1–19. doi:10.1177/00368504211023665.

[82] Milovac D, Weigand I, Kovačić M, et al. Highly porous hydroxyapatite derived from cuttlefish bone as TiO2 catalyst support. Process Appl Ceram. 2018;12(2):136–142.

[83] Rojas-Mayorga CK, Bonilla-Petriciolet A, Silvestre-Albero J, et al. Physico-chemical characterization of metal-doped bone chars and their adsorption behavior for water defluoridation. Appl Surf Sci. 2015;355:748–760. doi:10.1016/j.apsusc.2015.07.163.

[84] Zúñiga-Muro NM, Bonilla-Petriciolet A, Mendoza-Castillo DI, et al. Fluoride adsorption properties of cerium-containing bone char. J Fluor Chem. 2017;197:63–73. doi:10.1016/j.jfluchem.2017.03.004.

[85] Hossini H, Darvishi Cheshmeh Soltani R, Safari M, et al. The application of a natural chitosan/bone char composite in adsorbing textile dyes from water. Chem Eng Commun. 2017;204(9):1082–1093. doi:10.1080/00986445.2017.1340274.

[86] Liu J, He L, Dong F, et al. The role of nano-sized manganese coatings on bone char in removing arsenic(V) from solution: implications for permeable reactive barrier technologies. Chemosphere. 2016;153:146–154. doi:10.1016/j.chemosphere.2016.03.044.

[87] Wang H, Luo P. Preparation, kinetics, and adsorption mechanism study of microcrystalline cellulose-modified bone char as an efficient Pb (II) adsorbent. Water Air Soil Pollut. 2020;231(7):328, doi:10.1007/s11270-020-04687-8.

[88] Soltani DCR, et al. Decontamination of arsenic(V)-contained liquid phase utilizing Fe3O4/bone char

nanocomposite encapsulated in chitosan biopolymer. Environ Sci Pollut Res. 2017;24(17):15157–15166. doi:10.1007/s11356-017-9128-9.

[89] Kim J, Hwang J, Choi Y, et al. Effects of pyrolysis temperature of the waste cattle bone char on the fluoride adsorption characteristics. J Korean Soc Water Wastewater. 2020;34(1):1–8. doi:10.11001/jksww.2020.34.1.001.

[90] Brunson LR, Sabatini DA. An evaluation of fish bone char as an appropriate arsenic and fluoride removal technology for emerging regions. Environ Eng Sci. 2009;26(12):1777–1784.

[91] Iriarte-Velasco U, Sierra I, Zudaire L, et al. Conversion of waste animal bones into porous hydroxyapatite by alkaline treatment: effect of the impregnation ratio and investigation of the activation mechanism. J Mater Sci. 2015;50(23):7568–7582. doi:10.1007/s10853-015-9312-6.

[92] Iriarte-Velasco U, Ayastuy JL, Zudaire L, et al. An insight into the reactions occurring during the chemical activation of bone char. Chem Eng J. 2014;251:217–227. doi:10.1016/j.cej.2014.04.048.

[93] Feng L, Xu W, Liu T, et al. Heat regeneration of hydroxyapatite/attapulgite composite beads for defluoridation of drinking water. J Hazard Mater. 2012;221–222:228–235. doi:10.1016/j.jhazmat.2012.04.040.

[94] Kaseva ME. Optimization of regenerated bone char for fluoride removal in drinking water: a case study in Tanzania. J Water Health. 2006;4(1):139–147. doi:10.2166/wh.2005.062.

[95] Nigri EM, Bhatnagar A, Rocha SDF. Thermal regeneration process of bone char used in the fluoride removal from aqueous solution. J Clean Prod. 2017;142:3558–3570. doi:10.1016/j.jclepro.2016.10.112.

[96] Herath HMAS, Kawakami T, Tafu M. Repeated heat regeneration of bone char for sustainable use in fluoride removal from drinking water. Healthcare. 2018;6(4):143, doi:10.3390/healthcare6040143.

[97] Nigri EM, Santos ALA, Bhatnagar A, et al. Chemical regeneration of bone char associated with a continuous system for defluoridation of water. Brazilian J Chem Eng. 2019;36(4):1631–1643. doi:10.1590/0104-6632.20190364s20180258.

[98] Kanyora A, Kinyanjui TK, Kariuki SM, et al. Efficiency of various sodium solutions in regeneration of fluoride saturated bone char for de-fluoridation. IOSR J Environ Sci Toxicol Food Technol. 2014;8(10):10–16. doi:10.9790/2402-081031016.

[99] Coltre DSC, Cionek AC, Meneguin GJ, et al. Study of dye desorption mechanism of bone char utilizing different regenerating agents. SN Appl Sci. 2020;2(12):1–14. doi:10.1007/s42452-020-03911-8.

[100] Jia P, Tan H, Liu K, et al. Synthesis and photocatalytic performance of ZnO/bone char composite. Materials (Basel. 2018;11(10):1–8. doi:10.3390/ma11101981.

[101] Jia P, Tan H, Liu K, et al. Synthesis, characterization and photocatalytic property of novel ZnO/bone char composite. Mater Res Bull. 2018;102(February):45–50. doi:10.1016/j.materresbull.2018.02.018.

[102] Rezaee A, Rangkooy H, Khavanin A, et al. High photocatalytic decomposition of the air pollutant formaldehyde using nano-ZnO on bone char. Environ Chem Lett. 2014;12(2):353–357. doi:10.1007/s10311-014-0453-7.